Exponentially Enhanced Light-Matter Interaction, Cooperativities, and Steady-State Entanglement Using Parametric Amplification

Wei Qin,[1,2] Adam Miranowicz,[2,3] Peng-Bo Li,[2,4] Xin-You Lü,[5] J. Q. You,[1,6] and Franco Nori[2,7]

[1]*Quantum Physics and Quantum Information Division, Beijing Computational Science Research Center, Beijing 100193, China*
[2]*CEMS, RIKEN, Wako-shi, Saitama 351-0198, Japan*
[3]*Faculty of Physics, Adam Mickiewicz University, 61-614 Poznań, Poland*
[4]*Shaanxi Province Key Laboratory of Quantum Information and Quantum Optoelectronic Devices,*
Department of Applied Physics, Xi'an Jiaotong University, Xi'an 710049, China
[5]*School of Physics, Huazhong University of Science and Technology, Wuhan 430074, China*
[6]*Department of Physics, Zhejiang University, Hangzhou 310027, China*
[7]*Physics Department, The University of Michigan, Ann Arbor, Michigan 48109-1040, USA*

We propose an experimentally feasible method for enhancing the atom-field coupling as well as the ratio between this coupling and dissipation (i.e., cooperativity) in an optical cavity. It exploits optical parametric amplification to exponentially enhance the atom-cavity interaction and, hence, the cooperativity of the system, with the squeezing-induced noise being completely eliminated. Consequently, the atom-cavity system can be driven from the weak-coupling regime to the strong-coupling regime for modest squeezing parameters, and even can achieve an effective cooperativity much larger than 100. Based on this, we further demonstrate the generation of steady-state nearly maximal quantum entanglement. The resulting entanglement infidelity (which quantifies the deviation of the actual state from a maximally entangled state) is exponentially smaller than the lower bound on the infidelities obtained in other dissipative entanglement preparations without applying squeezing. In principle, we can make an arbitrarily small infidelity. Our generic method for enhancing atom-cavity interaction and cooperativities can be implemented in a wide range of physical systems, and it can provide diverse applications for quantum information processing.

Cavity [1] and circuit [2,3] quantum electrodynamics (QED) provide promising platforms to implement light-matter interactions at the single-particle level by efficiently coupling single atoms to quantized cavity fields. Exploiting such coupled systems for quantum information processing often requires the strong-coupling regime (SCR), where the atom-cavity coupling g exceeds both atomic spontaneous-emission rate γ and cavity-decay rate κ, such that a single excitation can be coherently exchanged between atom and cavity before their coherence is lost. A typical parameter quantifying this property is the cooperativity defined as $C = g^2/(\kappa\gamma)$. Experimentally, microwave systems (like quantum superconducting circuits) can have very high cooperativities of order up to 10^4 [3–5]. However, for most optical systems (see [6] for a notable exception in photonic band gap cavities), it is currently challenging to achieve the SCR and, in particular, the cooperativity of C larger than 10^2 [7–12]. This directly limits the ability to process quantum information in optical cavities. Here, we propose a novel approach for this problem, and we demonstrate that the light-matter coupling and cooperativity can be exponentially increased with a cavity squeezing parameter. Specifically, we parametrically squeeze the cavity mode to strengthen the coherent coupling g, and at

the same time, we apply a broadband squeezed-vacuum field to completely eliminate the noise induced by squeezing. As an intriguing application, we show how to improve exponentially the quality of steady-state entanglement.

Quantum entanglement is not only a striking feature of quantum physics but also a fundamental resource in quantum information technologies. The preparation of an entangled state between atoms in optical cavities can be directly implemented using controlled unitary dynamics [13,14]. However, the presence of an atomic spontaneous emission and cavity loss leads to a poor infidelity scaling $\delta = (1 - \mathcal{F}) \propto 1/\sqrt{C}$ [15], where $\mathcal{F}$ is the fidelity, which characterizes the distance between the ideal and actual states, and δ is the corresponding infidelity. This is owing to the fact that both decays can carry away information about the system and destroy its coherence. For this reason, many approaches, which have been proposed for entanglement preparation, are focused on dissipation engineering, which treats dissipative processes as a resource rather than as a detrimental noise [16–23]. In the resulting entanglement, the infidelity scaling has a quadratic improvement, $\delta \propto 1/C$ [24–30]. Such an infidelity, however, remains lower-bounded by the cooperativity, because only partial dissipation contributes to the entanglement, which still suffers
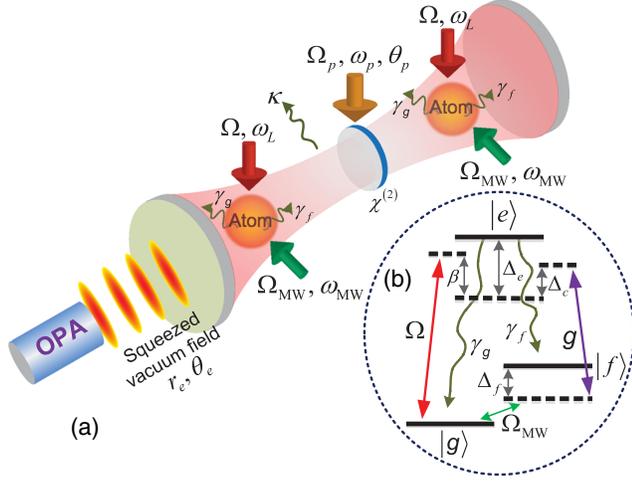
FIG. 1. Schematics of the proposed method for enhancing cooperativity and maximizing steady-state entanglement. (a) Two driven atoms are trapped inside a single-mode cavity, which contains a $\chi^{(2)}$ nonlinear medium strongly pumped at amplitude Ω_p, frequency ω_p, and phase θ_p. The cavity couples to a squeezed-vacuum reservoir, which is generated by optical parametric amplification (OPA) with a squeezing parameter r_e and a reference phase θ_e. As depicted in (b), the three-level atoms (in the Λ configuration) are coupled to the cavity mode with a strength g. In addition, the transition with Rabi frequency Ω (Ω_{MW}) is driven by a laser (microwave) field of frequency ω_L (ω_{MW}). We also assume that, along with a cavity decay rate κ, the excited state $|e\rangle$ of the atoms decays to the ground states $|g\rangle$ and $|f\rangle$ at rates γ_g and γ_f, respectively.

errors from other kinds (or channels) of dissipation. In this Letter, we demonstrate that our approach for the cooperativity enhancement can lead to an exponential suppression of undesired dissipation and, as a consequence, of the entanglement infidelity. Since the discussed model is generic, our proposal can be realized in a wide range of physical systems, in particular, optical cavities.

Basic idea.—As depicted in Fig. 1(a), we consider a quantum system consisting of two Λ atoms and a $\chi^{(2)}$ nonlinear medium. The atoms are confined in a single-mode cavity of frequency ω_c. The ground states of each atom, $|g\rangle$ and $|f\rangle$, are excited to the state $|e\rangle$, respectively, via a laser drive with Rabi frequency Ω and the coupling to the cavity mode with strength g, as shown in Fig. 1(b). If the nonlinear medium is pumped (say, at frequency ω_p, amplitude Ω_p, and phase θ_p), then the cavity mode can be squeezed along the axis rotated at the angle $(\pi - \theta_p)/2$. When Ω_p is close to the detuning $\Delta_c = \omega_c - \omega_p/2$, the atom-cavity coupling can be enhanced exponentially with a controllable squeezing parameter $r_p = (1/4) \ln [(1 + \alpha)/(1 - \alpha)]$, where $\alpha = \Omega_p/\Delta_c$. Meanwhile, squeezing the cavity mode also induces thermal noise and two-photon correlations in the cavity. In order to suppress them, a possible strategy is to use the squeezed vacuum field to drive the cavity [31–36]. This causes the squeezed-cavity

mode to equivalently interact with the thermal vacuum reservoir, and therefore, it yields an effective cooperativity exhibiting an exponential enhancement with $2r_p$.

Furthermore, to generate steady-state entanglement, we tune the squeezed-cavity mode to resonantly drive the transition $|f\rangle \rightarrow |e\rangle$, and as a result, the excitation-number-nonconserving processes would be strongly suppressed. Thus, in the limit of $\Omega \ll g_s$, the ground-state subspace, spanned by $\{|\phi_\pm\rangle = (|gg\rangle \pm |ff\rangle)|0\rangle_s/\sqrt{2}$, $|\psi_\pm\rangle = (|gf\rangle \pm |fg\rangle)|0\rangle_s/\sqrt{2}\}$, is decoupled from all of the excited states except the dark state, $|D\rangle = (|fe\rangle - |ef\rangle)|0\rangle_s/\sqrt{2}$, from the atom-cavity interaction. Here, the number refers to the squeezed-cavity photon number. For entanglement preparation, in order to be independent of an initial state, we apply an off-resonant microwave field of frequency ω_{MW} to couple $|g\rangle$ and $|f\rangle$ with the Rabi frequency Ω_{MW}, as shown in Fig. 1(b), to drive the transitions $|\phi_-\rangle \rightarrow |\phi_+\rangle \rightarrow |\psi_+\rangle$. Subsequently, the laser drive Ω excites $|\psi_+\rangle$ to $|D\rangle$, which then decays to $|\psi_-\rangle$ via atomic spontaneous emission. The populations initially in the ground-state subspace are, thus, driven to and trapped in $|\psi_-\rangle$, resulting in a maximally-entangled steady state, the singlet state $|S\rangle = (|gf\rangle - |fg\rangle)/\sqrt{2}$, between the atoms. In contrast to previous proposals of entanglement preparation that relied on the unitary or dissipative dynamics, and where the entanglement infidelities were lower-bounded by the system cooperativities [15,24–28], our approach can, in principle, make the entanglement infidelity arbitrarily small by increasing the squeezing parameter of the cavity mode for a modest value of the cooperativity.

Enhanced light-matter interaction and cooperativity.— Specifically, in a proper observation frame, the Hamiltonian determining the unitary dynamics of the system reads (hereafter, we set $\hbar = 1$)

$$H(t) = \sum_k (\Delta_e |e\rangle_k \langle e| + \Delta_f |f\rangle_k \langle f|) + H_{NL} + H_{AC}$$
$$+ \frac{1}{2}\Omega_{MW} \sum_k (|f\rangle_k \langle g| + \text{H.c.}) + V(t). \quad (1)$$

Here, $k = 1$, 2 labels the atoms, $H_{NL} = \Delta_c a^\dagger a + \frac{1}{2}\Omega_p(e^{i\theta_p}a^2 + \text{H.c.})$ is the nonlinear Hamiltonian for degenerate parametric amplification, $H_{AC} = g\sum_k(a|e\rangle_k\langle f| + \text{H.c.})$ is the atom-cavity coupling Hamiltonian, and $V(t) = \frac{1}{2}\Omega e^{i\beta t}\sum_k[(-1)^{k-1}|g\rangle_k\langle e| + \text{H.c.}]$ describes the interaction of a classical laser drive with the atoms. The detunings are $\Delta_e = \omega_e - \omega_g - \omega_{MW} - \omega_p/2$, $\Delta_f = \omega_f - \omega_g - \omega_{MW}$, and $\beta = \omega_L - \omega_{MW} - \omega_p/2$, where ω_L is the laser frequency of the atom drive and ω_z is the frequency associated with level $|z\rangle$ ($z = g$, f, e). Upon introducing the Bogoliubov squeezing transformation $a_s = \cosh(r_p)a + \exp(-i\theta_p)\sinh(r_p)a^\dagger$ [37], H_{NL} is diagonalized to $H_{NL} = \omega_s a_s^\dagger a_s$, where $\omega_s = \Delta_c\sqrt{1 - \alpha^2}$ is

the squeezed-cavity frequency. The atom-cavity coupling Hamiltonian likewise becomes $H_{AC} = \sum_k [(g_s a_s - g'_s a^{\dagger}_s)|e\rangle_k \langle f| + \text{H.c.}]$, with $g_s = g \cosh(r_p)$ and $g'_s = \exp(-i\theta_p) g \sinh(r_p)$. The excitation-number-nonconserving processes originating from the counter-rotating terms of the form $a^{\dagger}_s \sum_k |e\rangle_k \langle f|$, and $a_s \sum_k |f\rangle_k \langle e|$ can be neglected under the assumption that $|g'_s|/(\omega_s + \Delta_e - \Delta_f) \ll 1$, corresponding to the rotating-wave approximation, such that H_{AC} is transformed to the Jaynes-Cummings Hamiltonian

$$H_{ASC} = g_s \sum_k (a_s |e\rangle_k \langle f| + \text{H.c.}), \quad (2)$$

given in terms of the coupling strength g_s between the atoms and the squeezed-cavity mode. Therefore for $r_p \geq 1$, we predict an *exponentially-enhanced atom-cavity coupling*,

$$\frac{g_s}{g} \sim \frac{1}{2} \exp(r_p), \quad (3)$$

as plotted in the inset of Fig. 2. This is because there are $\sim \exp(2r_p)$ photons converted into a single-photon state, $|1\rangle_s$, of the squeezed-cavity mode. Such an exponential enhancement of this light-matter interaction is one of our most important results.

This squeezing also introduces additional noise into the cavity, as mentioned in the description above. To circumvent such undesired noises, a squeezed-vacuum field, with a squeezing parameter r_e and a reference phase θ_e, is used to drive the cavity [see Fig. 1(a)]. We consider the case where such a field has a much larger linewidth than the cavity mode. Indeed, a squeezing bandwidth of up to $\sim$GHz has been experimentally demonstrated via optical parametric amplification [38–40]. Because the linewidth is $\sim$MHz for typical optical cavities, we can think of this cavity drive as a squeezed reservoir. Hence, by ensuring $r_e = r_p$ and $\theta_e + \theta_p = \pm n\pi$ $(n = 1, 3, 5, \cdots)$, this additional noise can be eliminated completely (see the Supplemental Material [41] for details). As a consequence, the squeezed-cavity mode is equivalently coupled to a thermal vacuum reservoir, so that we can use the standard Lindblad operator to describe the cavity decay, yielding $L_{as} = \sqrt{\kappa} a_s$ with κ a decay rate. Similarly, atomic spontaneous emission is also described with the Lindblad operators $L_{g1} = \sqrt{\gamma_g}|g\rangle_1 \langle e|$, $L_{f1} = \sqrt{\gamma_f}|f\rangle_1 \langle e|$, $L_{g2} = \sqrt{\gamma_g}|g\rangle_2 \langle e|$, and $L_{f2} = \sqrt{\gamma_f}|f\rangle_2 \langle e|$. Here, we have assumed that in each atom, $|e\rangle$ decays to $|g\rangle$ and $|f\rangle$, respectively, with rates γ_g and γ_f. The dynamics of the atom-cavity system is, thus, governed by the standard master equation in the Lindblad form $\dot{\rho}(t) = i[\rho(t), H_s(t)] - \frac{1}{2}\sum_n \mathcal{L}(L_n)\rho(t)$, where $\rho(t)$ is the density operator of the system, $H_s(t)$ is given by $H(t)$ but with a $(a^{\dagger})$ replaced by a_s $(a^{\dagger}_s)$, and with H_{AC} replaced by H_{ASC}. Moreover, $\mathcal{L}(o)\rho = o^{\dagger}o\rho - 2o\rho o^{\dagger} + \rho o^{\dagger}o$ and
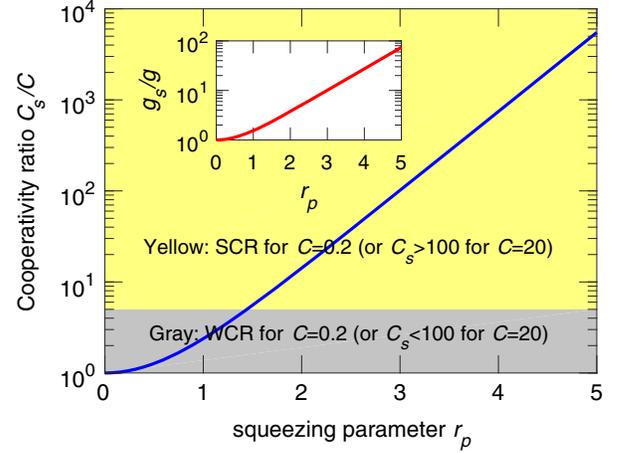

FIG. 2. Cooperativity enhancement C_s/C versus the squeezing parameter r_p. For $C = 0.2$, the gray and yellow shaded areas represent the WCR ($C_s < 1$) and the SCR ($C_s > 1$), respectively. For $C = 20$, the two shaded areas represent the regions, respectively, with $C_s < 100$ and $C_s > 100$. The inset shows the exponentially-enhanced effective coupling, g_s, between atom and cavity.

the sum runs over all dissipative processes mentioned above. We find that the above master equation gives an effective cooperativity $C_s = g_s^2/(\kappa\gamma)$. Consequently, increasing r_p enables an exponential enhancement in the atom-cavity coupling, given in Eq. (3), and thus, the cooperativity enhancement,

$$\frac{C_s}{C} \sim \frac{1}{4} \exp(2r_p), \quad (4)$$

as shown in Fig. 2. Note that our approach can exponentially strengthen the coherent coupling between atom and cavity, but *does not introduce any additional noise* into the system. It is seen in Fig. 2 that the atom-cavity system can be driven from the weak-coupling regime (WCR) to the SCR, e.g., with $C = 0.2$ and $r_p \geq 1.5$. Moreover, an effective cooperativity of $C_s > 10^2$ can also be achieved with modest C and r_p, e.g., $C = 20$ and $r_p \geq 1.5$. As one of many possible applications in quantum information technologies, this enhancement in the cooperativity (or coherent atom-field coupling) can be employed to improve the fidelity of dissipative entanglement preparation.

Maximizing steady-state entanglement.—Let us consider a weak drive Ω, so that the dominant dynamics of the system is restricted to a subspace having, at most, one excitation, and we can treat $V(t)$ as a perturbation to the system [46]. After adiabatically eliminating the excited states, the effective Hamiltonian is given by $H_{eff} = \Delta_f(\mathcal{I}/2 - |\phi_+\rangle\langle\phi_-| + \text{H.c.}) + \Omega_{MW}(|\psi_+\rangle\langle\phi_+| + \text{H.c.})$, where $\mathcal{I}$ is an identity operator acting on the ground manifold of the atoms. This implies that the microwave field can drive the population from $|\phi_+\rangle$ (or $|\phi_-\rangle$) to $|\psi_+\rangle$. Upon choosing $\Delta_e = \beta = \omega_s + \Delta_f$, the population in $|\psi_+\rangle$ is transferred to

$|\psi_-\rangle$ via the resonant drive and then the atomic spontaneous emission, which is mediated by the dark state $|D\rangle$. At the same time, the transition from $|\psi_-\rangle$ to the excited state of $|\varphi_e\rangle = (|fe\rangle + |ef\rangle)|0\rangle_s/\sqrt{2}$ is off-resonant, and it is negligible when $\Omega \ll g_s$. In this case, the rates of the effective decays into and out of the desired state $|\psi_-\rangle = |S\rangle|0\rangle_s$ are expressed, respectively, as $\Gamma_{in} = (\Omega/2)^2[4\gamma_g/\gamma^2 + 4/(\gamma C_s) + \gamma_f/(2\gamma^2 C_s^2)]$ and $\Gamma_{out} = (\Omega/2)^2[1/(\gamma C_s) + (\gamma + \gamma_f)/(16\gamma^2 C_s^2)]$ (see the Supplemental Material [41] for a detailed derivation). Here, $\gamma = \gamma_g + \gamma_f$ is the total atomic decay rate. In the steady state, the entanglement infidelity can be expressed as $\delta \sim 1/[1 + \Gamma_{in}/(3\Gamma_{out})]$, which is reduced to $\delta \sim 3\gamma/(4\gamma_g C_s)$ for $C_s \gg 1$. Further, as long as $r_p \geq 1$, we directly obtain

$$\delta \sim \frac{3\gamma}{\gamma_g \exp(2r_p)C}. \tag{5}$$

This explicitly shows an exponential improvement over the infidelity in the case of previous entanglement preparation protocols relying on engineered dissipation. The parametrically-enhanced cooperativity enables the entanglement infidelity to be very close to zero even for a modest value of C, rather than lower-bounded by $1/\sqrt{C}$ and $1/C$ [see Fig. 3(a)]. For the cooperativity values, which are easily accessible in current experiments, an entanglement infidelity of up to $\delta \sim 10^{-3}$ can be generated at a time $t = 200/\gamma$, as shown in Fig. 3(b). Note that, by increasing the driving laser strength Ω, the population transfer into the desired state is faster and, then, the infidelity is smaller for a given preparation time. However, at the same time, a nonadiabatic error increases with Ω, causing an increase in the infidelity. Thus, these are two competing processes. In addition, a larger C can more strongly reduce this nonadiabatic error and, therefore, lead to a smaller optimal driving strength [see Fig. 3(b)]. In a realistic setup based on ultracold ^{87}Rb atoms coupled to a Fabry-Perot resonator as discussed below [11], an atomic linewidth of $\gamma/2\pi = 3$ MHz and the cooperativity of $C = 42$ could result in $\delta \sim 1.2 \times 10^{-3}$, together with $t \sim 11$ μs, which allows us to neglect atomic decoherence.

We now consider the counter-rotating terms. In the limit $|g'_s|/\Delta_e \ll 1$, we find that such terms cause an energy shift of $|g'_s|^2/(2\Delta_e)$ to be imposed on the ground states and a coherent coupling, of strength $|g'_s|^2/(2\Delta_e)$, between the states $|\phi_+\rangle$ and $|\phi_-\rangle$ [47]. To remove these detrimental effects, the detunings need to be modified as $\Delta_e = \beta - |g'_s|^2/(2\Delta_e) = \omega_s + \Delta_f - |g'_s|^2/\Delta_e$ and $\Delta_f = \Omega_{MW}/\sqrt{2} + |g'_s|^2/(2\Delta_e)$, according to the analysis given in the Supplemental Material [41]. In this situation, the full system can be mapped to a simplified system that excludes the counter-rotating terms and has been discussed above. We numerically integrate the full master equation with the modified detunings [48,49], and find that, as in Fig. 3(a),
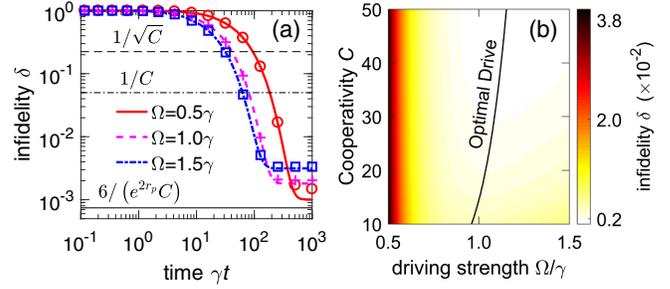

FIG. 3. (a) Evolution of the entanglement infidelity δ for different driving strengths $\Omega = 0.5\gamma$, 1.0γ, and 1.5γ, with the cooperativity $C = 20$. We assumed $\Delta_f = \Omega/2^{7/4}$ and $\Delta_f = \Omega/2^{7/4} + |g'_s|^2/(2\Delta_e)$, $\Delta_e = 200g'_s$ when using the effective (thick curves) and full (symbols) master equations, respectively. This yields an excellent agreement especially for time $t \in [0, 500/\gamma]$. The steady-state error decreases as Ω and becomes closer to $6/(e^{2r_p}C)$ (thin solid line), far below both $1/\sqrt{C}$ (thin dashed line) and $1/C$ (thin dotted-dashed line). (b) Entanglement infidelity at $t = 200/\gamma$ as a function of C and Ω. Here, due to excellent agreement between our predictions based on the full and effective master equations in panel (a), only the latter equation was used in panel (b). The solid line represents the optimal drive resulting in the smallest error for a given cooperativity. In both plots, we have assumed that $\gamma_g = \gamma/2$, $\kappa = 2\gamma/3$, $\Omega_{MW} = \sqrt{2}\Delta_f$, $r_p = 3$, $\theta_p = \pi$, while the initial state of the atoms is $(\mathcal{I} - |\psi_-\rangle\langle\psi_-|)/3$ and the cavity is initially in the vacuum.

the exact entanglement infidelity is in excellent agreement with the prediction of the effective dynamics during a very long time interval (e.g., $0 \leq t \leq 500/\gamma$).

Possible implementations.—We consider a possible experimental implementation utilizing ultracold ^{87}Rb atoms trapped in a high-finesse Fabry-Perot resonator [11]. Here, the ^{87}Rb atoms are used for the Λ-configuration atoms, and the Fabry-Perot resonator works as the single-mode cavity. When focusing on electric-dipole transitions of the D_1 line at a wavelength of 795 nm, we choose $|g\rangle \equiv |F = 1, m_F = -1\rangle$, $|f\rangle \equiv |F = 2, m_F = -2\rangle$, and $|e\rangle \equiv |F' = 2, m'_F = -2\rangle$, where $F^{(\prime)}$ and $m_F^{(\prime)}$ are quantum numbers characterizing the Zeeman states in the manifolds $5S_{1/2}$ ($5P_{1/2}$). In this situation, a circularly σ^--polarized control laser and a π-polarized-cavity mode are needed to couple the transitions $|F = 1, m_F = -1\rangle \rightarrow$ and $|F = 2, m_F = -2\rangle \rightarrow |F' = 2, m'_F = -2\rangle$, respectively. For the two ground states, although their electric-dipole transition is forbidden due to their same parity, a microwave field could directly couple these states through the magnetic-dipole interaction. Such a coupling has experimentally reached values of hundreds of kHz [50,51]. Moreover, the cavity mode can be squeezed typically using, e.g., a periodically-poled KTiOPO$_4$ (PPKTP) crystal [52–54]. In order to generate a squeezed-vacuum reservoir, we can also use a PPKTP crystal with a high-bandwidth pump, so the squeezing bandwidth of up to $\sim$GHz [38,39] is possible.

Solid-state implementations can be considered in the context of nitrogen-vacancy (NV) centers in diamond with a whispering-gallery-mode (WGM) microresonator [7]. In this setup, the electronic spin states of the NV centers are used to form the Λ-configuration structures, such that $|g\rangle \equiv |^3A_2, m_s = -1\rangle$, $|f\rangle \equiv |^3A_2, m_s = +1\rangle$, and $|e\rangle \equiv (|E_-, m_s = +1\rangle + |E_+, m_s = -1\rangle)/\sqrt{2}$. The NV spins have extremely long coherence times at room temperature, while the WGM microresonators made out of nonlinear crystals exhibit strong optical nonlinearities [55,56]. These are the key requirements for the entanglement preparation with a weak atom drive and a squeezed-cavity mode.

As an alternative example of solid-state system, the proposed method of maximizing steady-state entanglement can also be realized in superconducting quantum circuits [57–59], where two flux or transmon qubits and a coplanar waveguide resonator are used [2,60]. A superconducting quantum interference device (SQUID) can be inserted into the resonator, which is able to create the squeezed vacuum in the resonator [31,61–65]. All required parts of such devices have been implemented in superconducting experiments [3].

Conclusions.—We have shown that parametric squeezing enables an exponential enhancement of both coherent coupling between an atom and a cavity, as well as the corresponding cooperativity. As a simple application, the steady-state entanglement preparation, which results in an exponentially better fidelity than previous dissipation-based protocols, has also been demonstrated here. In principle, our method can be extended to other local quantum operations, e.g., many-body entanglement preparation [28,66] and quantum gate implementations [29,67–70]. We suggest to use squeezed light for only performing local intracavity quantum operations and to turn it off for converting stationary qubits into flying qubits. Moreover, due to a controllable squeezed-cavity frequency, the present method should enable reaching the ultra-SCR in optical cavities. Thus, one may observe many interesting phenomena in cavity-QED, similar to those observed in circuit QED [3,71–73]. Indeed, in particular for optical cavities, enhancing the light-matter interaction and cooperativities is of both fundamental and practical importance, so we expect that this technique could find diverse applications in quantum technologies [74,75].

[1] S. Haroche and J.-M. Raimond, *Exploring the Quantum: Atoms, Cavities, and Photons* (Oxford University Press, Oxford, 2006).

[2] J. Q. You and F. Nori, Atomic physics and quantum optics using superconducting circuits, Nature (London) **474**, 589 (2011).

[3] X. Gu, A. F. Kockum, A. Miranowicz, Y.-x. Liu, and F. Nori, Microwave photonics with superconducting quantum circuits, Phys. Rep. **718–719**, 1 (2017).

[4] R. J. Schoelkopf and S. M. Girvin, Wiring up quantum systems, Nature (London) **451**, 664 (2008).

[5] Z. L. Xiang, S. Ashhab, J. Q. You, and F. Nori, Hybrid quantum circuits: Superconducting circuits interacting with other quantum systems, Rev. Mod. Phys. **85**, 623 (2013).

[6] B. Lev, K. Srinivasan, P. Barclay, O. Painter, and H. Mabuchi, Feasibility of detecting single atoms using photonic bandgap cavities, Nanotechnology **15**, S556 (2004).

[7] Y. Park, A. K. Cook, and H. Wang, Cavity QED with diamond nanocrystals and silica microspheres, Nano Lett. **6**, 2075 (2006).

[8] J. D. Thompson, T. G. Tiecke, N. P. de Leon, J. Feist, A. V. Akimov, M. Gullans, A. S. Zibrov, V. Vuletić, and M. D. Lukin, Coupling a single trapped atom to a nanoscale optical cavity, Science **340**, 1202 (2013).

[9] I. Shomroni, S. Rosenblum, Y. Lovsky, O. Bechler, G. Guendelman, and B. Dayan, All-optical routing of single photons by a one-atom switch controlled by a single photon, Science **345**, 903 (2014).

[10] S. Kato and T. Aoki, Strong Coupling between a Trapped Single Atom and an All-Fiber Cavity, Phys. Rev. Lett. **115**, 093603 (2015).

[11] C. Hamsen, K. N. Tolazzi, T. Wilk, and G. Rempe, Two-Photon Blockade in an Atom-Driven Cavity QED System, Phys. Rev. Lett. **118**, 133604 (2017).

[12] S. Welte, B. Hacker, S. Daiss, S. Ritter, and G. Rempe, Cavity Carving of Atomic Bell States, Phys. Rev. Lett. **118**, 210503 (2017).

[13] T. Pellizzari, S. A. Gardiner, J. I. Cirac, and P. Zoller, Decoherence, Continuous Observation, and Quantum Computing: A Cavity QED Model, Phys. Rev. Lett. **75**, 3788 (1995).

[14] S.-B. Zheng and G.-C. Guo, Efficient Scheme for Two-Atom Entanglement and Quantum Information Processing in Cavity QED, Phys. Rev. Lett. **85**, 2392 (2000).

[15] A. S. Sørensen and K. Mølmer, Measurement Induced Entanglement and Quantum Computation with Atoms in Optical Cavities, Phys. Rev. Lett. **91**, 097905 (2003).

[16] S. Bose, P. L. Knight, M. B. Plenio, and V. Vedral, Proposal for Teleportation of an Atomic State via Cavity Decay, Phys. Rev. Lett. **83**, 5158 (1999).

[17] G. Chimczak, R. Tanaś, and A. Miranowicz, Teleportation with insurance of an entangled atomic state via cavity decay, Phys. Rev. A **71**, 032316 (2005).

[18] B. Kraus, H. P. Büchler, S. Diehl, A. Kantian, A. Micheli, and P. Zoller, Preparation of entangled states by quantum Markov processes, Phys. Rev. A 78, 042307 (2008).

[19] F. Verstraete, M. M. Wolf, and J. I. Cirac, Quantum computation and quantum-state engineering driven by dissipation, Nat. Phys. 5, 633 (2009).

[20] H. Krauter, C. A. Muschik, K. Jensen, W. Wasilewski, J. M. Petersen, J. I. Cirac, and E. S. Polzik, Entanglement Generated by Dissipation and Steady State Entanglement of Two Macroscopic Objects, Phys. Rev. Lett. 107, 080503 (2011).

[21] D. K. Burgarth, P. Facchi, V. Giovannetti, H. Nakazato, S. Pascazio, and K. Yuasa, Exponential rise of dynamical complexity in quantum computing through projections, Nat. Commun. 5, 5173 (2014).

[22] I. Yusipov, T. Laptyeva, S. Denisov, and M. Ivanchenko, Localization in Open Quantum Systems, Phys. Rev. Lett. 118, 070402 (2017).

[23] M. Hartmann, D. Poletti, M. Ivanchenko, S. Denisov, and P. Hänggi, Asymptotic Floquet states of open quantum systems: The role of interaction, New J. Phys. 19, 083011 (2017).

[24] M. J. Kastoryano, F. Reiter, and A. S. Sørensen, Dissipative Preparation of Entanglement in Optical Cavities, Phys. Rev. Lett. 106, 090502 (2011).

[25] L.-T. Shen, X.-Y. Chen, Z.-B. Yang, H.-Z. Wu, and S.-B. Zheng, Steady-state entanglement for distant atoms by dissipation in coupled cavities, Phys. Rev. A 84, 064302 (2011).

[26] Y. Lin, J. P. Gaebler, F. Reiter, T. R. Tan, R. Bowler, A. S. Sørensen, D. Leibfried, and D. J. Wineland, Dissipative production of a maximally entangled steady state of two quantum bits, Nature (London) 504, 415 (2013).

[27] S.-L. Su, X.-Q. Shao, H.-F. Wang, and S. Zhang, Scheme for entanglement generation in an atom-cavity system via dissipation, Phys. Rev. A 90, 054302 (2014).

[28] F. Reiter, D. Reeb, and A. S. Sørensen, Scalable Dissipative Preparation of Many-Body Entanglement, Phys. Rev. Lett. 117, 040501 (2016).

[29] J. Borregaard, P. Komar, E. M. Kessler, A. S. Sørensen, and M. D. Lukin, Heralded Quantum Gates with Integrated Error Detection in Optical Cavities, Phys. Rev. Lett. 114, 110502 (2015).

[30] W. Qin, X. Wang, A. Miranowicz, Z. Zhong, and F. Nori, Heralded quantum controlled-phase gates with dissipative dynamics in macroscopically distant resonators, Phys. Rev. A 96, 012315 (2017).

[31] K. W. Murch, S. J. Weber, K. M. Beck, E. Ginossar, and I. Siddiqi, Reduction of the radiative decay of atomic coherence in squeezed vacuum, Nature (London) 499, 62 (2013).

[32] M. Bartkowiak, L.-A. Wu, and A. Miranowicz, Quantum circuits for amplification of Kerr nonlinearity via quadrature squeezing, J. Phys. B 47, 145501 (2014).

[33] X.-Y. Lü, Y. Wu, J. R. Johansson, H. Jing, J. Zhang, and F. Nori, Squeezed Optomechanics with Phase-Matched Amplification and Dissipation, Phys. Rev. Lett. 114, 093602 (2015).

[34] M. Lemonde, N. Didier, and A. A. Clerk, Enhanced nonlinear interactions in quantum optomechanics via mechanical amplification, Nat. Commun. 7, 11338 (2016).

[35] J. B. Clark, F. Lecocq, R. W. Simmonds, J. Aumentado, and J. D. Teufel, Sideband cooling beyond the quantum backaction limit with squeezed light, Nature (London) 541, 191 (2017).

[36] S. Zeytinoğlu, A. İmamoğlu, and S. Huber, Engineering Matter Interactions Using Squeezed Vacuum, Phys. Rev. X 7, 021041 (2017).

[37] M. O. Scully and M. S. Zubairy, Quantum Optics (Cambridge University Press, Cambridge, 1997).

[38] S. Ast, M. Mehmet, and R. Schnabel, High-bandwidth squeezed light at 1550 nm from a compact monolithic PPKTP cavity, Opt. Express 21, 13572 (2013).

[39] T. Serikawa, J. Yoshikawa, K. Makino, and A. Furusawa, Creation and measurement of broadband squeezed vacuum from a ring optical parametric oscillator, Opt. Express 24, 28383 (2016).

[40] C. F. Ockeloen-Korppi, E. Damskägg, J.-M. Pirkkalainen, T. T. Heikkilä, F. Massel, and M. A. Sillanpää, Noiseless Quantum Measurement and Squeezing of Microwave Fields Utilizing Mechanical Vibrations, Phys. Rev. Lett. 118, 103601 (2017).

[41] See Supplemental Material at http://link.aps.org/supplemental/10.1103/PhysRevLett.120.093601 for detailed derivations of our main results, which includes Refs. [41–44].

[42] M. Stefszky, R. Ricken, C. Eigner, V. Quiring, H. Herrmann, and C. Silberhorn, Waveguide Cavity Resonator as a Source of Optical Squeezing, Phys. Rev. Applied 7, 044026 (2017).

[43] F. Mallet, M. A. Castellanos-Beltran, H. S. Ku, S. Glancy, E. Knill, K. D. Irwin, G. C. Hilton, L. R. Vale, and K. W. Lehnert, Quantum State Tomography of an Itinerant Squeezed Microwave Field, Phys. Rev. Lett. 106, 220502 (2011).

[44] D. M. Toyli, A. W. Eddins, S. Boutin, S. Puri, D. Hover, V. Bolkhovsky, W. D. Oliver, A. Blais, and I. Siddiqi, Resonance Fluorescence from an Artificial Atom in Squeezed Vacuum, Phys. Rev. X 6, 031004 (2016).

[45] M. A. Castellanos-Beltran, K. D. Irwin, G. C. Hilton, L. R. Vale, and K. W. Lehnert, Amplification and squeezing of quantum noise with a tunable Josephson metamaterial, Nat. Phys. 4, 929 (2008).

[46] F. Reiter and A. S. Sørensen, Effective operator formalism for open quantum systems, Phys. Rev. A 85, 032111 (2012).

[47] O. Gamel and D. F. V James, Time-averaged quantum dynamics and the validity of the effective hamiltonian model, Phys. Rev. A 82, 052106 (2010).

[48] J. R. Johansson, P. D. Nation, and F. Nori, Qutip: An opensource Python framework for the dynamics of open quantum systems, Comput. Phys. Commun. 183, 1760 (2012).

[49] J. R. Johansson, P. D. Nation, and F. Nori, Qutip 2: A Python framework for the dynamics of open quantum systems, Comput. Phys. Commun. 184, 1234 (2013).

[50] P. Treutlein, T. Steinmetz, Y. Colombe, B. Lev, P. Hommelhoff, J. Reichel, M. Greiner, O. Mandel, A. Widera, T. Rom, I. Bloch, and T. W. Hänsch, Quantum information processing in optical lattices and magnetic microtraps, Fortschr. Phys. 54, 702 (2006).

[51] L. Sárkány, P. Weiss, H. Hattermann, and J. Fortágh, Controlling the magnetic-field sensitivity of atomic-clock

states by microwave dressing, Phys. Rev. A **90,** 053416 (2014).

[52] H. Vahlbruch, M. Mehmet, S. Chelkowski, B. Hage, A. Franzen, N. Lastzka, S. Goßler, K. Danzmann, and R. Schnabel, Observation of Squeezed Light with 10-dB Quantum-Noise Reduction, Phys. Rev. Lett. **100,** 033602 (2008).

[53] H. Vahlbruch, M. Mehmet, K. Danzmann, and R. Schnabel, Detection of 15 dB Squeezed States of Light and Their Application for the Absolute Calibration of Photoelectric Quantum Efficiency, Phys. Rev. Lett. **117,** 110801 (2016).

[54] R. Schnabel, Squeezed states of light and their applications in laser interferometers, Phys. Rep. **684,** 1 (2017).

[55] J. U. Fürst, D. V. Strekalov, D. Elser, A. Aiello, U. L. Andersen, C. Marquardt, and G. Leuchs, Quantum Light from a Whispering-Gallery-Mode Disk Resonator, Phys. Rev. Lett. **106,** 113901 (2011).

[56] F. Sedlmeir, M. R. Foreman, U. Vogl, R. Zeltner, G. Schunk, D. V. Strekalov, C. Marquardt, G. Leuchs, and H. G. L. Schwefel, Polarization-Selective Out-Coupling of Whispering-Gallery Modes, Phys. Rev. Applied **7,** 024029 (2017).

[57] J. Q. You and F. Nori, Superconducting circuits and quantum information, Phys. Today **58,** 42 (2005).

[58] S. O. Valenzuela, W. D. Oliver, D. M. Berns, K. K. Berggren, L. S. Levitov, and T. P. Orlando, Microwave-induced cooling of a superconducting qubit, Science **314,** 1589 (2006).

[59] J. Q. You, Y.-x. Liu, and F. Nori, Simultaneous Cooling of an Artificial Atom and its Neighboring Quantum System, Phys. Rev. Lett. **100,** 047001 (2008).

[60] T. Yamamoto, K. Inomata, K. Koshino, P. M. Billangeon, Y. Nakamura, and J. S. Tsai, Superconducting flux qubit capacitively coupled to an LC resonator, New J. Phys. **16,** 015017 (2014).

[61] K. Moon and S. M. Girvin, Theory of Microwave Parametric Down-Conversion and Squeezing Using Circuit QED, Phys. Rev. Lett. **95,** 140504 (2005).

[62] A. M. Zagoskin, E. Il'ichev, M. W. McCutcheon, J. F. Young, and F. Nori, Controlled Generation of Squeezed States of Microwave Radiation in a Superconducting Resonant Circuit, Phys. Rev. Lett. **101,** 253602 (2008).

[63] L. Zhong, E. P. Menzel, R. Di Candia, P. Eder, M. Ihmig, A. Baust, M. Haeberlein, E. Hoffmann, K. Inomata, T. Yamamoto, Y. Nakamura, E. Solano, F. Deppe, A. Marx,

and R. Gross, Squeezing with a flux-driven Josephson parametric amplifier, New J. Phys. **15,** 125013 (2013).

[64] S. Kono, Y. Masuyama, T. Ishikawa, Y. Tabuchi, R. Yamazaki, K. Usami, K. Koshino, and Y. Nakamura, Non-classical Photon Number Distribution in a Superconducting Cavity under a Squeezed Drive, Phys. Rev. Lett. **119,** 023602 (2017).

[65] A. Bienfait, P. Campagne-Ibarcq, A. H. Kiilerich, X. Zhou, S. Probst, J. J. Pla, T. Schenkel, D. Vion, D. Esteve, J. J. L. Morton, K. Moelmer, and P. Bertet, Magnetic Resonance with Squeezed Microwaves, Phys. Rev. X **7,** 041011 (2017).

[66] L. Amico, R. Fazio, A. Osterloh, and V. Vedral, Entanglement in many-body systems, Rev. Mod. Phys. **80,** 517 (2008).

[67] L.-M. Duan and H. J. Kimble, Scalable Photonic Quantum Computation through Cavity-Assisted Interactions, Phys. Rev. Lett. **92,** 127902 (2004).

[68] J. Majer, J. M. Chow, J. M. Gambetta, J. Koch, B. R. Johnson, J. A. Schreier, L. Frunzio, D. I. Schuster, A. A. Houck, A. Wallraff, A. Blais, M. H. Devoret, S. M. Girvin, and R. J. Schoelkopf, Coupling superconducting qubits via a cavity bus, Nature (London) **449,** 443 (2007).

[69] A. Reiserer, N. Kalb, G. Rempe, and S. Ritter, A quantum gate between a flying optical photon and a single trapped atom, Nature (London) **508,** 237 (2014).

[70] B. Hacker, S. Welte, G. Rempe, and S. Ritter, A photon–photon quantum gate based on a single atom in an optical resonator, Nature (London) **536,** 193 (2016).

[71] L. Garziano, V. Macrì, R. Stassi, O. Di Stefano, F. Nori, and S. Savasta, One Photon Can Simultaneously Excite Two or More Atoms, Phys. Rev. Lett. **117,** 043601 (2016).

[72] A. F. Kockum, A. Miranowicz, V. Macrì, S. Savasta, and F. Nori, Deterministic quantum nonlinear optics with single atoms and virtual photons, Phys. Rev. A **95,** 063849 (2017).

[73] R. Stassi, V. Macrì, A. F. Kockum, O. Di Stefano, A. Miranowicz, S. Savasta, and F. Nori, Quantum nonlinear optics without photons, Phys. Rev. A **96,** 023818 (2017).

[74] I. Buluta, S. Ashhab, and F. Nori, Natural and artificial atoms for quantum computation, Rep. Prog. Phys. **74,** 104401 (2011).

[75] A. Reiserer and G. Rempe, Cavity-based quantum networks with single atoms and optical photons, Rev. Mod. Phys. **87,** 1379 (2015).

Wei Qin,[1,2] Adam Miranowicz,[2,3] Peng-Bo Li,[2,4] Xin-You Lü,[5] J. Q. You,[1,6] and Franco Nori[2,7]

[1]*Quantum Physics and Quantum Information Division,*
Beijing Computational Science Research Center, Beijing 100193, China
[2]*CEMS, RIKEN, Wako-shi, Saitama 351-0198, Japan*
[3]*Faculty of Physics, Adam Mickiewicz University, 61-614 Poznań, Poland*
[4]*Shaanxi Province Key Laboratory of Quantum Information and Quantum Optoelectronic Devices,*
Department of Applied Physics, Xi'an Jiaotong University, Xi'an 710049, China
[5]*School of Physics, Huazhong University of Science and Technology, Wuhan 430074, China*
[6]*Department of Physics, Zhejiang University, Hangzhou 310027, China*
[7]*Physics Department, The University of Michigan, Ann Arbor, Michigan 48109-1040, USA*

In this Supplemental Material to the article on "Exponentially-Enhanced Light-Matter Interaction, Cooperativities, and Steady-State Entanglement Using Parametric Amplification", we first present more details of the elimination of squeezing-induced noises to show an exponential enhancement of the light-matter interaction, as well as of the cooperativity. Then, we derive an effective master equation including an effective Hamiltonian and effective Lindblad operators, and also give a detailed description of our entanglement preparation method. Finally, we discuss, in detail, the effects of counter-rotating terms and show how to remove them.

S1. Elimination of squeezing-induced fluctuation noise

To demonstrate more explicitly the elimination of the squeezing-induced noise, we now derive the Lindblad master equation for our atom-cavity system. In addition to an exponential enhancement of the atom-cavity coupling, the squeezing can introduce undesired noise, including thermal noise and two-photon correlations, into the cavity mode. In order to avoid such noises, our approach employs an auxiliary, high-bandwidth squeezed-vacuum field, which can be experimentally generated, e.g., via optical parametric amplification [S1, S2]. Owing to the bandwidth of the squeezed-vacuum field of up to $\sim$ GHz, the auxiliary field can be thought of as a squeezed-vacuum reservoir for a typical cavity mode with its bandwidth of order of MHz. When being coupled to the cavity mode, the auxiliary field can suppress or even completely eliminate these undesired types of noise of the squeezed-cavity mode.

The Hamiltonian determining the unitary dynamics of our atom-cavity system, as shown in Fig. 1, is given by Eq. (1) and, for convenience, is recalled here

$$H\left(t\right) = \sum_{k}\left[\Delta_{e}|e\rangle_{k}\langle e| + \Delta_{f}|f\rangle_{k}\langle f|\right] + H_{\mathrm{AC}} + H_{\mathrm{NL}}$$
$$+ \frac{1}{2}\Omega_{\mathrm{MW}}\sum_{k}\left(|f\rangle_{k}\langle g| + \mathrm{H.c.}\right) + V\left(t\right), \tag{S1}$$

$$H_{\mathrm{NL}} = \Delta_{c}a^{\dagger}a + \frac{1}{2}\Omega_{p}\left[\exp\left(i\theta_{p}\right)a^{2} + \mathrm{H.c.}\right], \tag{S2}$$

$$H_{\mathrm{AC}} = g\sum_{k}\left(a|e\rangle_{k}\langle f| + \mathrm{H.c.}\right), \tag{S3}$$

$$V\left(t\right) = \frac{1}{2}\Omega\exp\left(i\beta t\right)\sum_{k}\left[\left(-1\right)^{k-1}|g\rangle_{k}\langle e| + \mathrm{H.c.}\right]. \tag{S4}$$

Here $k = 1, 2$ labels the atoms, g is the atom-cavity coupling, the annihilation operator a corresponds to the cavity mode, Ω (Ω_{MW}) is the Rabi frequency of the laser (microwave) drive applied to the atoms, and Ω_{p} (θ_{p}) is the amplitude (phase) of the strong pump applied to the nonlinear medium. We have defined the following detunings:

$$\Delta_{c} = \omega_{c} - \omega_{p}/2, \tag{S5}$$
$$\Delta_{e} = \omega_{e} - \omega_{g} - \omega_{\mathrm{MW}} - \omega_{p}/2, \tag{S6}$$
$$\Delta_{f} = \omega_{f} - \omega_{g} - \omega_{\mathrm{MW}}, \tag{S7}$$
$$\beta = \omega_{L} - \omega_{\mathrm{MW}} - \omega_{p}/2, \tag{S8}$$

where ω_c is the cavity frequency, ω_L (ω_{MW}) is the frequency of the laser (microwave) drive applied to the atoms, ω_p is the frequency of the strong pump applied to the nonlinear medium, and ω_z is the frequency associated with level $|z\rangle$ ($z = g, f, e$). When the cavity mode is coupled to the squeezed-vacuum reservoir with a squeezing parameter r_e and a reference phase θ_e, the dynamics of the atom-cavity system is described by the following master equation [S3]:

$$\dot{\rho}(t) = i[\rho(t), H(t)] - \frac{1}{2}\left\{ \sum_{x'} \mathcal{L}(L_{x'})\rho(t) + (N+1)\mathcal{L}(L_a)\rho(t) \right.$$

$$\left. + N\mathcal{L}(L_a^\dagger)\rho(t) - M\mathcal{L}'(L_a)\rho(t) - M^*\mathcal{L}'(L_a^\dagger)\rho(t) \right\}, \tag{S9}$$

where $\rho(t)$ is the density operator of the system, a Lindblad operator $L_a = \sqrt{\kappa}a$ describes the cavity decay with a rate κ, and

$$N = \sinh^2(r_e) \quad \text{and} \quad M = \cosh(r_e)\sinh(r_e)e^{-i\theta_e} \tag{S10}$$

describe thermal noise and two-photon correlations caused by the squeezed-vacuum reservoir, respectively. Moreover,

$$\mathcal{L}(o)\rho(t) = o^\dagger o\rho(t) - 2o\rho(t)o^\dagger + \rho(t)o^\dagger o, \tag{S11}$$

$$\mathcal{L}'(o)\rho(t) = oo\rho(t) - 2o\rho(t)o + \rho(t)oo \tag{S12}$$

and the sum runs over all atomic spontaneous emissions, including the Lindblad operators

$$L_{g1} = \sqrt{\gamma_g}|g\rangle_1\langle e|, \quad L_{f1} = \sqrt{\gamma_f}|f\rangle_1\langle e|, \quad L_{g2} = \sqrt{\gamma_g}|g\rangle_2\langle e|, \quad L_{f2} = \sqrt{\gamma_f}|f\rangle_2\langle e|. \tag{S13}$$

Note that, here, we have assumed that the atoms are coupled to a thermal reservoir and that in each atom, $|e\rangle$ decays to $|g\rangle$ and $|f\rangle$, respectively, with rates γ_g and γ_f.

When pumped, the nonlinear medium can squeeze the cavity mode along the axis rotated at an angle $(\pi - \theta_p)/2$, with a squeezing parameter $r_p = (1/4)\ln[(1+\alpha)/(1-\alpha)]$, where $\alpha = \Omega_p/\Delta_c$. This results in a squeezed-cavity mode, as described by the Bogoliubov transformation $a_s = \cosh(r_p)a + \exp(-i\theta_p)\sinh(r_p)a^\dagger$ [S3], such that

$$H_{\mathrm{NL}} = \omega_s a_s^\dagger a_s, \tag{S14}$$

where $\omega_s = \Delta_c\sqrt{1-\alpha^2}$ is the squeezed-cavity frequency. In terms of the mode a_s, the atom-cavity interaction Hamiltonian H_{AC} in Eq. (S3) is reexpressed as

$$H_{\mathrm{AC}} = \sum_k \left[\left(g_s a_s - g_s' a_s^\dagger\right)|e\rangle_k\langle f| + \mathrm{H.c.} \right], \tag{S15}$$

where $g_s = g\cosh(r_p)$ and $g_s' = \exp(-i\theta_p)g\sinh(r_p)$. Under the assumption that $|g_s'|/(\omega_s + \Delta_e - \Delta_f) \ll 1$, we can make the rotating-wave approximation to neglect the counter-rotating terms, which results in a standard Jaynes-Cummings Hamiltonian

$$H_{\mathrm{ASC}} = g_s \sum_k (a_s|e\rangle_k\langle f| + \mathrm{H.c.}). \tag{S16}$$

This Hamiltonian describes an interaction between the atoms and the squeezed-cavity mode, and demonstrate that as long as $r_p \geq 1$, there is an exponential enhancement in the atom-cavity coupling,

$$\frac{g_s}{g} \sim \frac{1}{2}\exp(r_p). \tag{S17}$$

Furthermore, the master equation in Eq. (S9) can accordingly be reexpressed as

$$\dot{\rho}(t) = i[\rho(t), H_s(t)]$$

$$- \frac{1}{2}\left\{ \sum_{x'} \mathcal{L}(L_{x'})\rho(t) + (N_s+1)\mathcal{L}(L_{as})\rho(t) \right.$$

$$\left. + N_s\mathcal{L}(L_{as}^\dagger)\rho(t) - M_s\mathcal{L}'(L_{as})\rho(t) - M_s^*\mathcal{L}'(L_{as}^\dagger)\rho(t) \right\}, \tag{S18}$$

$$H_s(t) = \sum_k [\Delta_e|e\rangle_k\langle e| + \Delta_f|f\rangle_k\langle f|] + \omega_s a_s^\dagger a_s + H_{\mathrm{ASC}}$$

$$+ \frac{1}{2}\Omega_{\mathrm{MW}} \sum_k (|f\rangle_k\langle g| + \mathrm{H.c.}) + V(t), \tag{S19}$$

where N_s and M_s are given, respectively, by

$$
\begin{aligned}
N_s = {}& \cosh^2\left(r_p\right)\sinh^2\left(r_e\right) + \sinh^2\left(r_p\right)\cosh^2\left(r_e\right) \\
& + \frac{1}{2}\sinh\left(2r_p\right)\sinh\left(2r_e\right)\cos\left(\theta_e + \theta_p\right),
\end{aligned}
\tag{S20}
$$

$$
\begin{aligned}
M_s = {}& \exp\left(i\theta_p\right)\left[\sinh\left(r_p\right)\cosh\left(r_e\right) + \exp\left[-i\left(\theta_e + \theta_p\right)\right]\cosh\left(r_p\right)\sinh\left(r_e\right)\right] \\
& \times \left[\cosh\left(r_p\right)\cosh\left(r_e\right) + \exp\left[i\left(\theta_p + \theta_e\right)\right]\sinh\left(r_e\right)\sinh\left(r_p\right)\right],
\end{aligned}
\tag{S21}
$$

corresponding to an effective thermal noise and two-photon correlations of the squeezed-cavity mode, and where $L_{as} = \sqrt{\kappa}a_s$ is a Lindblad operator corresponding to the decay of the squeezed-cavity mode, $g_s = g\cosh\left(r_p\right)$ is the enhanced, controllable atom-cavity coupling. We have neglected the counter-rotating terms to obtain the Hamiltonian H_s. From Eqs. (S20) and (S21), we can, as $r_e = 0$, observe the noise caused only by squeezing the cavity mode. However, when choosing $r_e = r_p$ and $\theta_e + \theta_p = \pm n\pi$ $(n = 1, 3, 5, \cdots)$, we have

$$
N_s = M_s = 0,
\tag{S22}
$$

so that the master equation is simplified to a Lindblad form,

$$
\dot{\rho}\left(t\right) = i\left[\rho\left(t\right), H_s\left(t\right)\right] - \frac{1}{2}\sum_x \mathcal{L}\left(L_x\right)\rho\left(t\right).
\tag{S23}
$$

Here, the sum runs over all dissipative processes, including atomic spontaneous emission and squeezed-cavity decay. From Eq. (S23), we find that the squeezed-cavity mode is equivalently coupled to a thermal reservoir, and the squeezing-induced noises are completely removed as desired. Therefore, we can define the effective cooperativity $C_s = g_s^2/\left(\kappa\gamma\right)$, and obtain an exponential enhancement in the atom-cavity cooperativity $C = g^2/\left(\kappa\gamma\right)$, that is,

$$
\frac{C_s}{C} = \cosh^2\left(r_p\right) \sim \frac{1}{4}\exp\left(2r_p\right).
\tag{S24}
$$

This can be used to improve the quality of dissipative entanglement preparation. The resulting entanglement infidelity is no longer lower-bounded by the cooperativity C of the atom-cavity system and could be, in principle, made very close to zero.

Our method is to use a squeezed-vacuum field to suppress the noise of the squeezed-cavity mode, including thermal noise and two-photon correlations. This makes the squeezed-cavity mode equivalently coupled to a thermal-vacuum reservoir. Therefore, this method only changes the environment of the squeezed-cavity mode, and cannot cause the cavity mode to violate the Heisenberg uncertainty principle. To elucidate more explicitly the physics underlying this effect and to obtain an analytical understanding, we consider a simple case when the cavity mode is decoupled from the atoms. In this case, the Hamiltonian only includes the nonlinear term given in Eq. (S2). The cavity mode is then coupled to the squeezed-vacuum reservoir. Following the same method as before, we can find that the squeezed-cavity mode is equivalently coupled to a thermal vacuum reservoir. The corresponding master equation is

$$
\dot{\rho}\left(t\right) = i\left[\rho\left(t\right), \omega_s a_s^\dagger a_s\right] - \frac{\kappa}{2}\left[a_s^\dagger a_s \rho\left(t\right) - 2a_s \rho\left(t\right)a_s^\dagger + \rho\left(t\right)a_s^\dagger a_s\right].
\tag{S25}
$$

We now calculate the Heisenberg uncertainty relation of the cavity mode a evolving according to the master equation given in Eq. (S25). To start, we define two rotated quadratures at an angle $\left(\pi - \theta_p\right)/2$,

$$
X_1 = \frac{1}{2}\left\{a\exp\left[-i\left(\pi - \theta_p\right)/2\right] + a^\dagger\exp\left[i\left(\pi - \theta_p\right)/2\right]\right\},
\tag{S26}
$$

$$
X_2 = \frac{1}{2i}\left\{a\exp\left[-i\left(\pi - \theta_p\right)/2\right] - a^\dagger\exp\left[i\left(\pi - \theta_p\right)/2\right]\right\}.
\tag{S27}
$$

In terms of the a_s mode, X_1 and X_2 can be reexpressed as

$$
X_1 = x_1 a_s + x_1^* a_s^\dagger,
\tag{S28}
$$

$$
X_2 = -i\left(x_2 a_s - x_2^* a_s^\dagger\right).
\tag{S29}
$$

Here,

$$
x_1 = \frac{1}{2}\left\{\exp\left[-i\left(\pi - \theta_p\right)/2\right]\cosh\left(r_p\right) - \exp\left[i\left(\pi + \theta_p\right)/2\right]\sinh\left(r_p\right)\right\},
\tag{S30}
$$

$$
x_2 = \frac{1}{2}\left\{\exp\left[-i\left(\pi - \theta_p\right)/2\right]\cosh\left(r_p\right) + \exp\left[i\left(\pi + \theta_p\right)/2\right]\sinh\left(r_p\right)\right\}.
\tag{S31}
$$

According to the master equation in Eq. (S25), a straightforward calculation gives

$$
\begin{aligned}
(\Delta X_1)^2 &= \langle X_1^2 \rangle - \langle X_1 \rangle^2 \\
&= \Big\{ y_1^2 \exp\left(-i2\omega_s t\right) \left[\langle a_s a_s \rangle(0) - \langle a_s \rangle^2(0) \right] \\
&\quad + 2|y_1|^2 \left[\langle a_s^\dagger a_s \rangle(0) - \langle a_s^\dagger \rangle(0) \langle a_s \rangle(0) \right] \\
&\quad + y_1^{*2} \exp\left(i2\omega_s t\right) \left[\langle a_s^\dagger a_s^\dagger \rangle(0) - \langle a_s^\dagger \rangle^2(0) \right] \Big\} \exp\left(-\kappa t\right) + \frac{1}{4} \exp\left(2r_p\right),
\end{aligned}
\tag{S32}
$$

$$
\begin{aligned}
(\Delta X_2)^2 &= \langle X_2^2 \rangle - \langle X_2 \rangle^2 \\
&= \Big\{ y_2^2 \exp\left(-i2\omega_s t\right) \left[\langle a_s \rangle^2(0) - \langle a_s a_s \rangle(0) \right] \\
&\quad + 2|y_2|^2 \left[\langle a_s^\dagger a_s \rangle(0) - \langle a_s^\dagger \rangle(0) \langle a_s \rangle(0) \right] \\
&\quad + y_2^{*2} \exp\left(i2\omega_s t\right) \left[\langle a_s^\dagger \rangle^2(0) \right] - \langle a_s^\dagger a_s^\dagger \rangle(0) \Big\} \exp\left(-\kappa t\right) + \frac{1}{4} \exp\left(-2r_p\right),
\end{aligned}
\tag{S33}
$$

where $\langle O \rangle(t)$ represents the expectation value of the operator O at the evolution time t. For simplicity, and without loss of generality, we assume that the squeezed-cavity mode is initially in a Fock state $|n_s\rangle$, with n_s being the squeezed-cavity photon number. In this case, we have

$$
(\Delta X_1)^2 = \frac{1}{4} \left[2n_s \exp\left(-\kappa t\right) + 1 \right] \exp\left(2r_p\right),
\tag{S34}
$$

$$
(\Delta X_2)^2 = \frac{1}{4} \left[2n_s \exp\left(-\kappa t\right) + 1 \right] \exp\left(-2r_p\right),
\tag{S35}
$$

and then

$$
(\Delta X_1)(\Delta X_2) = \frac{1}{4} \left[2n_s \exp\left(-\kappa t\right) + 1 \right] \geq \frac{1}{4}.
\tag{S36}
$$

It is found, from Eq. (S36), that the Heisenberg uncertainty relation holds, as expected.

We now turn to the discussion of the squeezed vacuum drive. The squeezing strength r_e and squeezing phase θ_e are experimentally adjustable quantities. In optics, the squeezed vacuum can be produced by a pumped $\chi^{(2)}$ nonlinear medium (e.g., a periodically-poled KTiOPO4 (PPKTP) crystal) placed in an optical cavity [S1, S2, S4, S5]. This method is similar to generating cavity-field squeezing of a atom-cavity system. The parameters r_e and θ_e can be controlled by the amplitude and phase of the laser, which pumps the crystal. To confirm the values of the parameters, one can further measure these by using balanced homodyne detection [S6]. The parameters r_p and θ_p can be controlled analogously in such a way to fulfill the conditions $r_e = r_p$ and $\theta_e + \theta_p = \pm n\pi$ $(n = 1, 3, 5, \cdots)$. We note that optical squeezing has also been experimentally implemented utilizing a waveguide cavity [S7].

Superconducting quantum circuits, due to their tunable nonlinearity and low losses for microwave fields, are other promising devices for producing squeezed states. The most popular method to generate microwave squeezing is to use a Josephson parametric amplifier (JPA) [S8–S12]. The JPA is a superconducting LC resonator, which consists of a superconducting quantum interference device (SQUID). This resonator can be pumped not only through the resonator, but also by modulating the magnetic flux in the SQUID. In this case, the parameters r_e and θ_e can be controlled by the amplitude and phase of a pump tone used to modulate the magnetic flux. Recent experiments have shown that the squeezed vacuum, generated by a JPA, can be used to reduce the radiative decay of superconducting qubits [S10] and to modify resonance fluorescence [S13]. The squeezing of quantum noise has also been demonstrated with tunable Josephson metamaterials [S14].

S2. Perturbative treatment and maximizing steady-state entanglement

For the preparation of a steady entangled state, e.g., the singlet state $|S\rangle = (|gf\rangle - |fg\rangle)/\sqrt{2}$, the key element is that the system dynamics cannot only drive the population into $|\psi_-\rangle$, but also prevent the population from moving out of $|\psi_-\rangle$. In our approach, when we choose $\Delta_e = \beta = \omega_s + \Delta_f$, the coherent couplings mediated by the laser drive and by the squeezed-cavity mode are resonant. In addition, the microwave field also resonantly drives the transition

$$
|\phi_-\rangle \leftrightarrow |\phi_+\rangle \leftrightarrow |\psi_+\rangle.
\tag{S37}
$$

The proposed entanglement preparation can, therefore, be understood via a hopping-like model, as illustrated in Fig. S1(a). Note that, here, Δ_f is required to be nonzero, or $|\phi_-\rangle$ becomes a dark state of the microwave drive, whose

population is trapped and cannot be transferred to $|\psi_+\rangle$. In the preparation process, the populations initially in the states $|\phi_-\rangle$, $|\phi_+\rangle$, and $|\psi_+\rangle$ can be coherently driven to the dark state $|D\rangle$ through the microwave and laser drives and, then, decay to the desired state $|\psi_-\rangle$ through two atomic decays, respectively, with rates γ_{g1} and γ_{g2}. Indeed, such atomic decays originate, respectively, from the spontaneous emissions, $|e\rangle \to |g\rangle$, of the two atoms, so we have $\gamma_{g1} = \gamma_{g2} = \gamma_g/4$. Furthermore, owing to the laser drive, the state $|\psi_-\rangle$ is resonantly excited to $|\varphi_e\rangle$. This state is then resonantly coupled to $|ff\rangle|1\rangle_s$ by the squeezed-cavity mode. The cavity loss causes the latter state to decay to $|ff\rangle|0\rangle_s$, thus giving rise to population leakage from $|\psi_-\rangle$. However, because of the exponential enhancement in the atom-cavity coupling [i.e., $g_s \sim g\exp(r_p)/2$ in Eq. (S17)], the state $|\varphi_e\rangle$ is split into a doublet of dressed states, $|e_\pm\rangle = (|\varphi_e\rangle \pm |ff\rangle|1\rangle_s)/\sqrt{2}$, exponentially separated by

$$2\sqrt{2}g_s \sim \sqrt{2}g\exp(r_p), \tag{S38}$$

which is much larger than the couplings strength $\Omega_\pm = \Omega/(2\sqrt{2})$, as shown in Fig. S1(b). Hence, the population leakage from $|\psi_-\rangle$ is exponentially suppressed, and we can make the effective decay rate, Γ_{out}, out of $|\psi_-\rangle$, exponentially smaller than the effective decay rate, Γ_{in}, into $|\psi_-\rangle$. To discuss these decay rates more specifically, we need to give an effective master equation of the system, when the laser drive Ω is assumed to be much smaller than the interactions inside the excited-state subspace. In this case, the coupling between the ground- and excited-state subspaces is treated as a perturbation, so that both cavity mode and excited states of the atoms can be adiabatically eliminated.
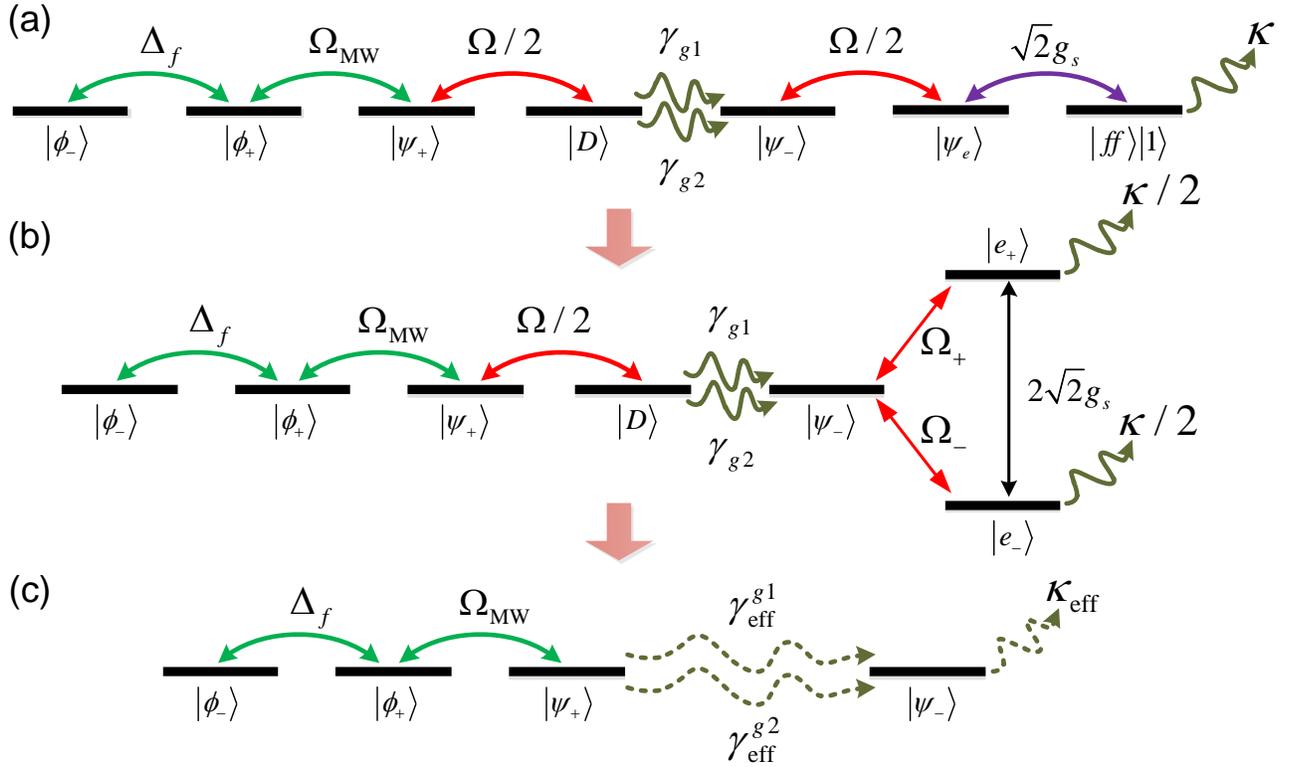

FIG. S1. (Color online) (a) Hopping-like model for the proposed steady-state nearly-maximal entanglement preparation. (b) Exponential suppression in the leakage of the population in $|\psi_-\rangle$. (c) Effective dynamics after adiabatically eliminating the states $|D\rangle$, $|e_+\rangle$, and $|e_-\rangle$.

Specifically, we follow the procedure in Ref. [S15], and begin by considering the Lindblad master equation in Eq. (S23). For convenience, we rewrite the Hamiltonian $H_s(t)$ as

$$H_s(t) = H_g + H_e + v(t) + v^\dagger(t), \tag{S39}$$

with

$$H_g = \sum_{k=1,2} \left[\Delta_f |f\rangle_k \langle f| + \frac{\Omega_{\mathrm{MW}}}{2} \left(|f\rangle_k \langle g| + \mathrm{H.c.} \right) \right], \tag{S40}$$

$$H_e = \sum_{k=1,2} |e\rangle_k \langle e| + \omega_s a_s^\dagger a_s + H_{\mathrm{ASC}}, \tag{S41}$$

representing the interactions, respectively, inside the ground- and excited-state subspaces, and

$$v(t) = \frac{1}{2} \exp\left(i\beta t \right) \Omega \sum_{k=1,2} \exp\left[i \left(k - 1 \right) \pi \right] |g\rangle_k \langle e| \tag{S42}$$

being the deexcitation from the excited-state subspace to the ground-states subspace. Under the assumption that the laser drive Ω is sufficiently weak compared to the coupling g_s, the effective Hamiltonian and Lindblad operators read:

$$H_{\mathrm{eff}} = -\frac{1}{2} \left[v(t) \left(H_{\mathrm{NH}} - \beta \right)^{-1} v^\dagger(t) \right] + H_g, \tag{S43}$$

$$L_{x,\mathrm{eff}} = L_x \left(H_{\mathrm{NH}} - \beta \right)^{-1} v^\dagger(t), \tag{S44}$$

where

$$H_{\mathrm{NH}} = H_e - \frac{i}{2} \sum_x L_x^\dagger L_x \tag{S45}$$

is the no-jump Hamiltonian. The system dynamics is, therefore, determined by an effective master equation

$$\dot{\rho}_g(t) = i \left[\rho_g(t), H_{\mathrm{eff}} \right] - \frac{1}{2} \sum_x \mathcal{L} \left(L_{x,\mathrm{eff}} \right) \rho_g(t), \tag{S46}$$

where $\rho_g(t)$ is the reduced density operator associated only with the ground states of the atoms. After a straightforward calculation restricted in the Hilbert space having at most one excitation, we have:

$$H_{\mathrm{eff}} = \Delta_f \left(\mathcal{I}/2 - |\phi_+\rangle\langle\phi_-| + \mathrm{H.c.} \right) + \Omega_{\mathrm{MW}} \left(|\psi_+\rangle\langle\phi_+| + \mathrm{H.c.} \right), \tag{S47}$$

$$L_{g1,\mathrm{eff}} = r_g \left[\left(|\psi_+\rangle + |\psi_-\rangle \right) \left(\gamma_{\mathrm{eff},0}\langle\psi_+| + \gamma_{\mathrm{eff},2}\langle\psi_-| \right) + \gamma_{\mathrm{eff},1} \left(|\phi_+\rangle + |\phi_-\rangle \right) \left(\langle\phi_+| + \langle\phi_-| \right) \right], \tag{S48}$$

$$L_{g2,\mathrm{eff}} = -r_g \left[\left(|\psi_+\rangle - |\psi_-\rangle \right) \left(\gamma_{\mathrm{eff},0}\langle\psi_+| - \gamma_{\mathrm{eff},2}\langle\psi_-| \right) + \gamma_{\mathrm{eff},1} \left(|\phi_+\rangle + |\phi_-\rangle \right) \left(\langle\phi_+| + \langle\phi_-| \right) \right], \tag{S49}$$

$$L_{f1,\mathrm{eff}} = r_f \left[\left(|\phi_+\rangle - |\phi_-\rangle \right) \left(\gamma_{\mathrm{eff},0}\langle\psi_+| + \gamma_{\mathrm{eff},2}\langle\psi_-| \right) + \gamma_{\mathrm{eff},1} \left(|\psi_+\rangle - |\psi_-\rangle \right) \left(\langle\phi_+| + \langle\phi_-| \right) \right], \tag{S50}$$

$$L_{f2,\mathrm{eff}} = -r_f \left[\left(|\phi_+\rangle - |\phi_-\rangle \right) \left(\gamma_{\mathrm{eff},0}\langle\psi_+| - \gamma_{\mathrm{eff},2}\langle\psi_-| \right) + \gamma_{\mathrm{eff},1} \left(|\psi_+\rangle + |\psi_-\rangle \right) \left(\langle\phi_+| + \langle\phi_-| \right) \right], \tag{S51}$$

$$L_{as,\mathrm{eff}} = r_{as} \left[\kappa_{\mathrm{eff},1} |\psi_-\rangle \left(\langle\phi_+| + \langle\phi_-| \right) - \frac{1}{\sqrt{2}} \kappa_{\mathrm{eff},2} \left(|\phi_+\rangle - |\phi_-\rangle \right) \langle\psi_-| \right]. \tag{S52}$$

Here,

$$\mathcal{I} = |\phi_+\rangle\langle\phi_+| + |\phi_-\rangle\langle\phi_-| + |\psi_+\rangle\langle\psi_+| + |\psi_-\rangle\langle\psi_-|, \tag{S53}$$

$$|\phi_\pm\rangle = \frac{1}{\sqrt{2}} \left(|gg\rangle \pm |ff\rangle \right), \tag{S54}$$

$$|\psi_\pm\rangle = \frac{1}{\sqrt{2}} \left(|gf\rangle \pm |fg\rangle \right), \tag{S55}$$

and

$$r_{g(f)} = \exp\left(-i\beta t \right) \frac{\Omega \sqrt{\gamma_{g(f)}}}{4\gamma}, \tag{S56}$$

$$r_{as} = \exp\left(-i\beta t \right) \frac{\Omega}{2\sqrt{\gamma}}, \tag{S57}$$

$$\gamma_{\mathrm{eff},0} = \frac{1}{\widetilde{\Delta}_{e,1}}, \tag{S58}$$

$$\gamma_{\mathrm{eff},m} = \frac{\widetilde{\omega}_{s,m}}{\widetilde{\omega}_{s,m}\widetilde{\Delta}_{e,m-1} - mC_s}, \tag{S59}$$

$$\kappa_{\mathrm{eff},m} = \frac{\sqrt{mC_s}}{\widetilde{\omega}_{s,m}\widetilde{\Delta}_{e,m-1} - mC_s}, \tag{S60}$$

where

$$\widetilde{\omega}_{s,m} = \frac{1}{\kappa} \left(\omega_s + m\Delta_f - \beta\right) - \frac{i}{2}, \tag{S61}$$

$$\widetilde{\Delta}_{e,m-1} = \frac{1}{\gamma} \left[\Delta_e + (m-1)\Delta_f - \beta\right] - \frac{i}{2}, \tag{S62}$$

for $m = 1, 2$, and where $\gamma = \gamma_g + \gamma_f$ is the total atomic decay rate.

Having obtained the effective master equation, let us now consider the decay rates Γ_{in} and Γ_{out}. According to the effective Lindblad operators in Eqs. (S48)-(S52), the decay rates of moving into and out of the singlet state $|\psi_-\rangle$ are given, respectively, by

$$\Gamma_{\text{in}} = \frac{\Omega^2}{4\gamma^2} \left(\gamma_g|\gamma_{\text{eff},0}|^2 + 2\gamma_f|\gamma_{\text{eff},1}|^2 + 4\gamma|\kappa_{\text{eff},1}|^2\right), \tag{S63}$$

$$\Gamma_{\text{out}} = \frac{\Omega^2}{4\gamma^2} \left(\gamma_g|\gamma_{\text{eff},2}|^2 + 2\gamma_f|\gamma_{\text{eff},2}|^2 + 2\gamma|\kappa_{\text{eff},2}|^2\right). \tag{S64}$$

Let us define the entanglement fidelity as $F = \langle\psi_-|\rho_g(t)|\psi_-\rangle$ (that is, the probability of the atoms being in $|\psi_-\rangle$) and, then, the entanglement infidelity as $\delta = 1 - F$. In the steady state $(t \to +\infty)$, the entanglement infidelity is found

$$\delta \sim \frac{1}{1 + \Gamma_{\text{in}}/(3\Gamma_{\text{out}})}. \tag{S65}$$

Note that, here, we have assumed that $|\phi_+\rangle$, $|\phi_-\rangle$, and $|\psi_+\rangle$ have the same population in a steady state. In order to prepare nearly-maximal steady-state entanglement, we choose the detunings to be

$$\Delta_e = \beta = \omega_s + \Delta_f, \tag{S66}$$

such that $\widetilde{\omega}_{s,m} \sim \widetilde{\Delta}_{e,m-1} \sim -i/2$, yielding

$$\frac{\Gamma_{\text{in}}}{\Gamma_{\text{out}}} \sim \frac{4\gamma_g}{\gamma} C_s \gg 1, \tag{S67}$$

for $C_s \gg 1$. As shown in Fig. S1(c), the underlying dynamics is as follows: after adiabatically eliminating the excited states $|D\rangle$, $|e_+\rangle$, and $|e_-\rangle$, the states $|\psi_+\rangle$ and $|\psi_-\rangle$ are directly connected by two effective spontaneous emission processes with rates γ_{eff}^{g1} and γ_{eff}^{g2},

$$\gamma_{\text{eff}}^{g1} = \gamma_{\text{eff}}^{g2} = |r_g\gamma_{\text{eff},0}|^2 \sim \frac{\gamma_g}{4\gamma^2}\Omega^2, \tag{S68}$$

and at the same time, the desired state $|\psi_-\rangle$ leaks the population through an effective cavity decay with a rate κ_{eff},

$$\kappa_{\text{eff}} = |r_{\text{as}}\kappa_{\text{eff},2}|^2/2 \sim \frac{\Omega^2}{16\gamma C_s}. \tag{S69}$$

Therefore, together with the effective Hamiltonian H_{eff} driving the populations from both $|\phi_+\rangle$ and $|\phi_-\rangle$ to $|\psi_+\rangle$, the initial populations in the ground-states subspace of the atoms can be transferred to $|\psi_-\rangle$ and trapped in this state. By substituting Eq. (S67) into Eq. (S65), we can straightforwardly have

$$\delta \sim \frac{3\gamma}{4\gamma_g C_s}. \tag{S70}$$

As long as $r_p \geq 1$, an exponential enhancement of the cooperativity, $C_s/C \sim \exp(2r_p)/4$, is obtained, leading to

$$\delta \sim \frac{3\gamma}{\gamma_g \exp(2r_p) C}. \tag{S71}$$

This equation shows that we can increase the squeezing parameter r_p, so as to exponentially decrease the entanglement infidelity, as seen in Fig. S2. Moreover, the result in this figure also reveals that, by decreasing Ω, one can suppress non-adiabatic errors and, thus, can cause the steady-state infidelity to approach a theoretical value, as expected. Hence, as opposed to prior entanglement preparation protocols, which relied on controlled unitary dynamics or engineered dissipation, such an infidelity is no longer lower bounded by the cooperativity C and, in principle, can be made very close to zero.
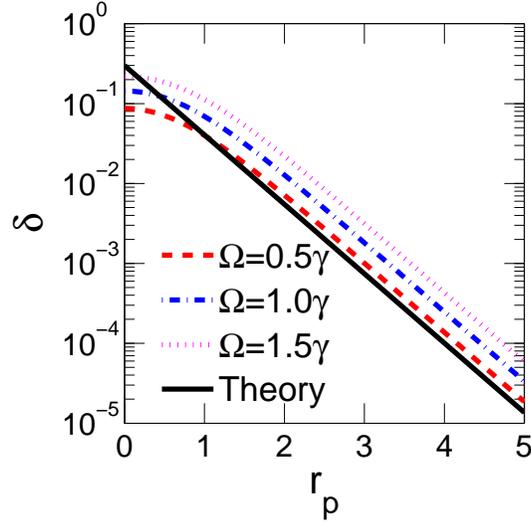
FIG. S2. (Color online) Steady-state entanglement infidelity versus the squeezing parameter r_p. We have plotted the numerical infidelity for $\Omega = 0.5\gamma$ (dashed curve), $\Omega = 1.0\gamma$ (dashed-dotted curve), and $\Omega = 1.5\gamma$ (dotted curve) by calculating the effective master equation, and also plotted the theoretical prediction (solid curve). Here, we have assumed that $\gamma_g = \gamma/2$, $\kappa = 2\gamma/3$, $C = 20$, $\Delta_f = \Omega/2^{7/4}$, $\Omega_{\mathrm{MW}} = \sqrt{2}\Delta_f$, and that with the vacuum cavity, the initial state of the atoms is $(\mathcal{I} - |\psi_-\rangle\langle\psi_-|)/3$.

S3. Effects of the counter-rotating terms

The counter-rotating terms of the form $a_s^\dagger \sum_k |e\rangle_k\langle f|$ and $a_s \sum_k |f\rangle_k\langle e|$, which result from optical parametric amplification, do not conserve the excitation number, and can couple the ground- and double-excited states subspaces. Thus, this would give rise to an additional leakage of the population in the desired state $|\psi_-\rangle$, and decrease the entanglement fidelity. For example, in the presence of the counter-rotating terms, the state $|\psi_-\rangle$ can be excited to a double-excitation state $(|ge\rangle - |eg\rangle)|1\rangle_s/\sqrt{2}$, which, then, de-excites to the ground state $|gg\rangle|0\rangle$ through cavity decay and spontaneous emission. In general, we can decrease the ratio $|g_s'|/(2\Delta_e)$ to reduce errors induced by these excitation-number-nonconserving processes. However, to reduce such errors more efficiently in the limit of $|g_s'|/(2\Delta_e)$, we analyze effects of counter-rotating terms, in detail, in this section, and demonstrate that by modifying external parameters, we can remove these terms and the full system can be mapped to a simplified system described above.

According to Eqs. (S14) and (S15), the full Hamiltonian of the system in the terms of the squeezed mode a_s is

$$
\begin{aligned}
H(t) = &\sum_k \left[\Delta_e |e\rangle_k\langle e| + \Delta_f |f\rangle_k\langle f|\right] + \omega_s a_s^\dagger a_s \\
&+ \sum_k \left[\left(g_s a_s - g_s' a_s^\dagger\right) |e\rangle_k\langle f| + \mathrm{H.c.}\right], \\
&+ \frac{1}{2}\Omega_{\mathrm{MW}} \sum_k \left(|f\rangle_k\langle g| + \mathrm{H.c.}\right) + V(t),
\end{aligned}
\tag{S72}
$$

$$
V(t) = \frac{1}{2}\Omega \exp(i\beta t) \sum_k \left[(-1)^{k-1} |g\rangle_k\langle e| + \mathrm{H.c.}\right].
\tag{S73}
$$

Indeed, the counter-rotating terms can be treated as the high-frequency components of the full Hamiltonian. In order to explicitly show these high-frequency components, we can express $H(t)$ into a rotating frame at

$$
H_0 = \Delta_e \sum_k |e\rangle_k\langle e| + (\omega_s + \Delta_f) a_s^\dagger a_s.
\tag{S74}
$$

Thus, $H(t)$ is transformed to

$$
\mathcal{H}(t) = \Delta_f \left(\sum_k |f\rangle_k\langle f| - a_s^\dagger a_s \right)
$$
$$
+ \sum_k \left(g_s a_s |e\rangle_k\langle f| - e^{i2\Delta_e t} g_s' a_s^\dagger |e\rangle_k\langle f| + \text{H.c.} \right)
$$
$$
+ \frac{1}{2}\Omega_{\text{MW}} \sum_k \left(|f\rangle_k\langle g| + \text{H.c.} \right) + \mathcal{V}, \tag{S75}
$$

$$
\mathcal{V} = \frac{1}{2}\Omega \sum_k \left[(-1)^{k-1} |g\rangle_k\langle e| + \text{H.c.} \right]. \tag{S76}
$$

Here, we have chosen $\Delta_e = \beta = \omega_s + \Delta_f$. Because Δ_f is required to be much smaller than Δ_e, $\mathcal{H}(t)$ can be divided into two parts, $\mathcal{H}(t) = H_{\text{low}} + H_{\text{high}}$, where

$$
H_{\text{low}} = \Delta_f \left(\sum_k |f\rangle_k\langle f| - a_s^\dagger a_s \right) + g_s \sum_k (a_s |e\rangle_k\langle f| + \text{H.c.})
$$
$$
+ \frac{1}{2}\Omega_{\text{MW}} \sum_k \left(|f\rangle_k\langle g| + \text{H.c.} \right) + \mathcal{V}, \tag{S77}
$$

$$
H_{\text{high}} = \sum_k \left(-e^{i2\Delta_e t} g_s' a_s^\dagger |e\rangle_k\langle f| + \text{H.c.} \right), \tag{S78}
$$

represent the low- and high- frequency components, respectively. Here, we consider the limit $|g_s'|/\Delta_e \ll 1$. By using a time-averaging treatment [S16], the behavior of H_{high} can be approximated by a time-averaged Hamiltonian,

$$
H_{\text{TA}} = \frac{|g_s'|^2}{2\Delta_e} \sum_k a_s^\dagger a_s \left(|e\rangle_k\langle e| - |f\rangle_k\langle f| \right)
$$
$$
- \frac{|g_s'|^2}{2\Delta_e} \sum_{k,k'} \left(|f\rangle_k\langle e| \right) \left(|e\rangle_{k'}\langle f| \right). \tag{S79}
$$

The first term describes an energy shift depending on the photon number of the squeezed-cavity mode, and the second term describes a direct coupling between the two atoms. Accordingly, $\mathcal{H}(t)$ becomes $\mathcal{H}(t) \simeq H_{\text{low}} + H_{\text{TA}}$, and after transforming back to the original frame, we obtain

$$
H(t) \simeq \sum_k \left[\Delta_e |e\rangle_k\langle e| + \Delta_f |f\rangle_k\langle f| \right] + \omega_s a_s^\dagger a_s
$$
$$
+ g_s \sum_k \left(a_s |e\rangle_k\langle f| + \text{H.c.} \right),
$$
$$
+ \frac{1}{2}\Omega_{\text{MW}} \sum_k \left(|f\rangle_k\langle g| + \text{H.c.} \right) + V(t) + H_{\text{TA}}. \tag{S80}
$$

We find, from Eq. (S79), that the counter-rotating terms are able to conserve the excitation number as long as $|g_s'|/\Delta_e \ll 1$. Therefore, we can restrict our discussion in a subspace having at most one excitation, as discussed above. In this subspace, H_{TA} is expanded as

$$
H_{\text{TA}} = -\frac{|g_s'|^2}{2\Delta_e} \left(\mathcal{I}/2 + |\varphi_e\rangle\langle\varphi_e| - |\phi_+\rangle\langle\phi_-| + \text{H.c.} \right)
$$
$$
- \frac{|g_s'|^2}{\Delta_e} \left(\mathcal{I}^{(1)}/2 - |\phi_+^{(1)}\rangle\langle\phi_-^{(1)}| + \text{H.c.} \right), \tag{S81}
$$

where

$$
\mathcal{I}^{(1)} = |\phi_+^{(1)}\rangle\langle\phi_+^{(1)}| + |\phi_-^{(1)}\rangle\langle\phi_-^{(1)}| + |\psi_+^{(1)}\rangle\langle\psi_+^{(1)}| + |\psi_-^{(1)}\rangle\langle\psi_-^{(1)}|,
$$
$$
|\phi_\pm^{(1)}\rangle = (|gg\rangle \pm |ff\rangle) |1\rangle_s/\sqrt{2},
$$
$$
|\psi_\pm^{(1)}\rangle = (|gf\rangle \pm |fg\rangle) |1\rangle_s/\sqrt{2}. \tag{S82}
$$

Equation (S81) indicates that the counter-rotating terms introduce an energy shift of $|g_s'|^2/(2\Delta_e)$ imposed upon the ground states, and a coherent coupling, of strength $|g_s'|^2/(2\Delta_e)$, between the states $|\phi_+\rangle$ and $|\phi_-\rangle$. From Fig. S1(a), we find that in the regime, where $\Omega/|g_s'|$ is comparable to $|g_s'|/\Delta_e$, such an energy shift can cause the $|\psi_+\rangle \to |D\rangle$ transition to become far off-resonant and, thus, suppress the population into the desired state $|\psi_-\rangle$. Meanwhile, this introduced coupling may increase the entanglement error originating from the microwave dressing of the ground states. For example, if $\Delta_f = |g_s'|^2/(2\Delta_e)$, then the state $|\phi_-\rangle$ becomes a dark state of the microwave drive. In this case, the population in $|\phi_-\rangle$ is trapped and cannot be transferred to $|\psi_-\rangle$. To remove these detrimental effects, it is essential to compensate this energy shift. According to the above analysis, the detunings in Eq. (S66) need to be modified as

$$\Delta_e = \beta - \frac{|g_s'|^2}{2\Delta_e} = \omega_s + \Delta_f - \frac{|g_s'|^2}{\Delta_e}. \tag{S83}$$

This modification simplifies the full dynamics to the same hopping-like model, as shown in Fig. S1(a) with $\Delta_f \to \Delta_f' = \Delta_f - |g_s|^2/(2\Delta_e)$. Therefore, we can map the full system to a simple system that excludes the counter-rotating terms and has been discussed above.
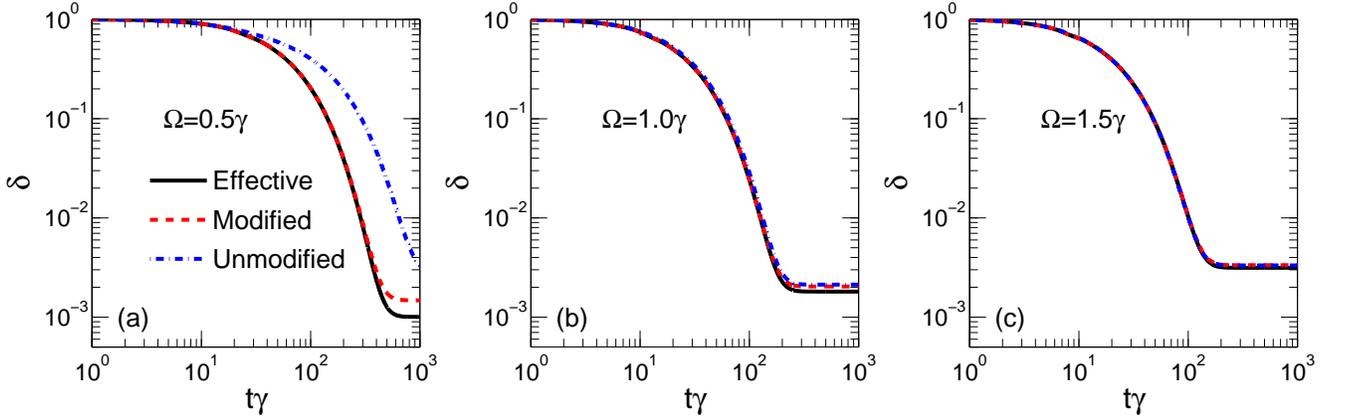

FIG. S3. (Color online) Entanglement infidelity δ as a function of time $t\gamma$ for (a) $\Omega = 0.5\gamma$, (b) $\Omega = 1.0\gamma$, and (c) $\Omega = 1.5\gamma$, assuming a cooperativity of $C = 20$. Solid and dashed-dotted curves are obtained, respectively, from integrations of the effective and full master equations, both with detunings $\Delta_f = \Omega/2^{7/4}$ and $\Delta_e = \beta = \omega_s + \Delta_f$. Dashed curves are also given by calculating the full master equation but with modified detunings $\Delta_f = \Omega/2^{7/4} + |g_s'|^2/(2\Delta_e)$ and $\Delta_e = \beta - |g_s'|^2/(2\Delta_e) = \omega_s + \Delta_f - |g_s'|^2/\Delta_e$. For both full cases, we have assumed $\Delta_e = 200g_s'$. In all plots, we have assumed that $\gamma_g = \gamma/2$, $\kappa = 2\gamma/3$, $\Omega_{\mathrm{MW}} = \sqrt{2}\Delta_f$, $r_p = 3$, and $\theta_p = \pi$. Moreover, the initial state of the atoms is $(\mathcal{I} - |\psi_-\rangle\langle\psi_-|)/3$ and the cavity was initially in the vacuum.

To understand this process better, we can follow the same method as above, but now with the Hamiltonian in Eq. (S80). Thus, we find the effective Hamiltonian and Lindblad operators as follows:

$$H_{\mathrm{eff}}' = \Delta_f' \left(\mathcal{I}/2 - |\phi_+\rangle\langle\phi_-| + \mathrm{H.c.}\right) + \Omega_{\mathrm{MW}} \left(|\psi_+\rangle\langle\phi_+| + \mathrm{H.c.}\right), \tag{S84}$$

$$L_{g1,\mathrm{eff}}' = r_g' \left[(|\psi_+\rangle + |\psi_-\rangle)\left(\gamma_{\mathrm{eff},0}'\langle\psi_+| + \gamma_{\mathrm{eff},2}'\langle\psi_-|\right) + \gamma_{\mathrm{eff},1}' \left(|\phi_+\rangle + |\phi_-\rangle\right)\left(\langle\phi_+| + \langle\phi_-|\right)\right], \tag{S85}$$

$$L_{g2,\mathrm{eff}}' = -r_g' \left[(|\psi_+\rangle - |\psi_-\rangle)\left(\gamma_{\mathrm{eff},0}'\langle\psi_+| - \gamma_{\mathrm{eff},2}'\langle\psi_-|\right) + \gamma_{\mathrm{eff},1}' \left(|\phi_+\rangle + |\phi_-\rangle\right)\left(\langle\phi_+| + \langle\phi_-|\right)\right], \tag{S86}$$

$$L_{f1,\mathrm{eff}}' = r_f' \left[(|\phi_+\rangle - |\phi_-\rangle)\left(\gamma_{\mathrm{eff},0}'\langle\psi_+| + \gamma_{\mathrm{eff},2}'\langle\psi_-|\right) + \gamma_{\mathrm{eff},1}' \left(|\psi_+\rangle - |\psi_-\rangle\right)\left(\langle\phi_+| + \langle\phi_-|\right)\right], \tag{S87}$$

$$L_{f2,\mathrm{eff}}' = -r_f' \left[(|\phi_+\rangle - |\phi_-\rangle)\left(\gamma_{\mathrm{eff},0}'\langle\psi_+| - \gamma_{\mathrm{eff},2}'\langle\psi_-|\right) + \gamma_{\mathrm{eff},1}' \left(|\psi_+\rangle + |\psi_-\rangle\right)\left(\langle\phi_+| + \langle\phi_-|\right)\right], \tag{S88}$$

$$L_{as,\mathrm{eff}}' = r_{as}' \left[\kappa_{\mathrm{eff},1}'|\psi_-\rangle\left(\langle\phi_+| + \langle\phi_-|\right) - \frac{1}{\sqrt{2}}\kappa_{\mathrm{eff},2}'\left(|\phi_+\rangle - |\phi_-\rangle\right)\langle\psi_-|\right]. \tag{S89}$$

Here,

$$\Delta_f' = \Delta_f - \frac{|g_s|^2}{2\Delta_e}, \tag{S90}$$

$$r_{g(f)}' = \exp(-i\beta t)\frac{\Omega\sqrt{\gamma_{g(f)}}}{4\gamma}, \tag{S91}$$

$$r_{as}' = \exp(-i\beta t)\frac{\Omega}{2\sqrt{\gamma}}, \tag{S92}$$

and

$$\gamma'_{\text{eff},0} = \frac{1}{\widetilde{\Delta}'_e}, \tag{S93}$$

$$\gamma'_{\text{eff},m} = \frac{\widetilde{\omega}'_{s,m}}{\widetilde{\omega}'_{s,m}\widetilde{\Delta}'_{e,m-1} - mC_s}, \tag{S94}$$

$$\kappa'_{\text{eff},m} = \frac{\sqrt{mC_s}}{\widetilde{\omega}'_{s,m}\widetilde{\Delta}'_{e,m-1} - mC_s} \tag{S95}$$

where

$$\widetilde{\Delta}'_e = (\Delta_e + \Delta_f - \beta)/\gamma - i/2, \tag{S96}$$

$$\widetilde{\omega}'_{s,m} = \left[\omega_s + m\left(\Delta_f - \frac{|g'_s|^2}{\Delta_e}\right) - \beta\right]/\kappa - i/2, \tag{S97}$$

$$\widetilde{\Delta}'_{e,m-1} = \left[\Delta_e - \beta + (m-1)\left(\Delta_f - \frac{|g'_s|^2}{\Delta_e}\right)\right]/\gamma - i/2, \tag{S98}$$

for $m = 1, 2$. Upon using the modified parameter, given in Eq. (S83), we obtain $\widetilde{\Delta}'_e \sim \widetilde{\omega}'_{s,m} \sim \widetilde{\Delta}'_{e,m-1} \sim -i/2$. This implies that the dynamics is the same as what we have already described for the simplified system without the counter-rotating terms, thereby leading to the same entanglement infidelity. To confirm this, we perform numerical calculations, as shown in Fig. S3. Specifically, we plot the entanglement infidelity as a function of rescaled time. Solid curves indicate the results obtained by integrating the effective master equation, whereas dashed and dashed-dotted curves reveal the predictions of the full master equation, respectively, with modified and unmodified detunings. These results demonstrate that the detrimental effects of the counter-rotating terms can be strongly suppressed by modifying external parameters, in particular, as what we have discussed above, for the case of weak Ω driving strengths, which are necessary for the validity of the perturbative treatment used in our approach.

[S1] S. Ast, M. Mehmet, and R. Schnabel, "High-bandwidth squeezed light at 1550 nm from a compact monolithic PPKTP cavity," Opt. Express 21, 13572–13579 (2013).
[S2] T. Serikawa, J. Yoshikawa, K. Makino, and A. Furusawa, "Creation and measurement of broadband squeezed vacuum from a ring optical parametric oscillator," Opt. Express 24, 28383–28391 (2016).
[S3] M. O. Scully and M. S. Zubairy, Quantum Optics (Cambridge University Press, Cambridge, 1997).
[S4] H. Vahlbruch, M. Mehmet, K. Danzmann, and R. Schnabel, "Detection of 15 dB squeezed states of light and their application for the absolute calibration of photoelectric quantum efficiency," Phys. Rev. Lett. 117, 110801 (2016).
[S5] H. Vahlbruch, M. Mehmet, S. Chelkowski, B. Hage, A. Franzen, N. Lastzka, S. Goßler, K. Danzmann, and R. Schnabel, "Observation of squeezed light with 10-dB quantum-noise reduction," Phys. Rev. Lett. 100, 033602 (2008).
[S6] R. Schnabel, "Squeezed states of light and their applications in laser interferometers," Phys. Rep. 684, 1–51 (2017).
[S7] M. Stefszky, R. Ricken, C. Eigner, V. Quiring, H. Herrmann, and C. Silberhorn, "Waveguide cavity resonator as a source of optical squeezing," Phys. Rev. Applied 7, 044026 (2017).
[S8] J. B. Clark, F. Lecocq, R. W. Simmonds, J. Aumentado, and J. D. Teufel, "Sideband cooling beyond the quantum backaction limit with squeezed light," Nature (London) 541, 191–195 (2017).
[S9] A. Bienfait, P. Campagne-Ibarcq, A. H. Kiilerich, X. Zhou, S. Probst, J. J. Pla, T. Schenkel, D. Vion, D. Esteve, J. J. L. Morton, K. Moelmer, and P. Bertet, "Magnetic resonance with squeezed microwaves," Phys. Rev. X 7, 041011 (2017).
[S10] K. W. Murch, S. J. Weber, K. M. Beck, E. Ginossar, and I. Siddiqi, "Reduction of the radiative decay of atomic coherence in squeezed vacuum." Nature (London) 499, 62–65 (2013).
[S11] L. Zhong, E. P. Menzel, R. Di Candia, P. Eder, M. Ihmig, A. Baust, M. Haeberlein, E. Hoffmann, K. Inomata, T. Yamamoto, Y. Nakamura, E. Solano, F. Deppe, A. Marx, and R. Gross, "Squeezing with a flux-driven Josephson parametric amplifier," New J. Phys. 15, 125013 (2013).
[S12] F. Mallet, M. A. Castellanos-Beltran, H. S. Ku, S. Glancy, E. Knill, K. D. Irwin, G. C. Hilton, L. R. Vale, and K. W. Lehnert, "Quantum state tomography of an itinerant squeezed microwave field," Phys. Rev. Lett. 106, 220502 (2011).
[S13] D. M. Toyli, A. W. Eddins, S. Boutin, S. Puri, D. Hover, V. Bolkhovsky, W. D. Oliver, A. Blais, and I. Siddiqi, "Resonance fluorescence from an artificial atom in squeezed vacuum," Phys. Rev. X 6, 031004 (2016).
[S14] M. A. Castellanos-Beltran, K. D. Irwin, G. C. Hilton, L. R. Vale, and K. W. Lehnert, "Amplification and squeezing of quantum noise with a tunable Josephson metamaterial," Nat. Phys. 4, 929–931 (2008).
[S15] F. Reiter and A. S. Sørensen, "Effective operator formalism for open quantum systems," Phys. Rev. A 85, 032111 (2012).
[S16] O. Gamel and D. F. V James, "Time-averaged quantum dynamics and the validity of the effective hamiltonian model," Phys. Rev. A 82, 052106 (2010).